Martian Moons Exploration MMX: Sample Return Mission to Phobos Elucidating Formation Processes of Habitable Planets

Kiyoshi Kuramoto (keikei@ep.sci.hokudai.ac.jp)
Hokkaido University https://orcid.org/0000-0002-6757-8064

Yasuhiro Kawakatsu
JAXA

Masaki Fujimoto
JAXA

Akito Araya
The University of Tokyo: Tokyo Daigaku

Maria Antonietta Barucci
Paris Observatory: Observatoire de Paris

Hidenori Genda
Tokyo Institute of Technology

Naru Hirata
The University of Aizu: Aizu Daigaku

Hitoshi Ikeda
JAXA

Takeshi Imamura
The University of Tokyo: Tokyo Daigaku

Jörn Helbert
Deutsches Zentrum fur Luft- und Raumfahrt DLR

Shingo Kameda
Rikkyo University

Masanori Kobayashi
Chiba Institute of Technology

Hiroki Kusano
National Institutes for Quantum and Radiological Science and Technology

David J. Lawrence
Johns Hopkins University Applied Physics Laboratory

Koji Matsumoto
National Astronomical Observatory of Japan

Patrick Michel

Universite Cote d'Azur
Hideaki Miyamoto
The University of Tokyo: Tokyo Daigaku
Tomokatsu Morota
The University of Tokyo: Tokyo Daigaku
Hiromu Nakagawa
Tohoku University: Tohoku Daigaku
Tomoki Nakamura
Tohoku University
Kazunori Ogawa
JAXA
Hisashi Otake
JAXA
Masanobu Ozaki
JAXA
Sara Russel
Natural History Museum
Sho Sasaki
Osaka University: Osaka Daigaku
Hirotaka Sawada
JAXA
Hiroki Senshu
Chiba Institute of Technology: Chiba Kogyo Daigaku
Shogo Tachibana
The University of Tokyo: Tokyo Daigaku
Naoki Terada
Tohoku University: Tohoku Daigaku
Stephan Ulamec
Deutsches Zentrum für Luft- und Raumfahrt DRL
Tomohiro Usui
JAXA
Koji Wada
Chiba Institute of Technology: Chiba Kogyo Daigaku
Sei-ichiro Watababe
Nagoya University: Nagoya Daigaku
Shoichiro Yokota
Osaka University: Osaka Daigaku

Frontier Letter (by invitation only)

Keywords: Phobos, Deimos, Mars, sample return mission, early solar system, habitable planet

Posted Date: February 3rd, 2021

DOI: https://doi.org/10.21203/rs.3.rs-163944/v1

Version of Record: A version of this preprint was published at Earth, Planets and Space on January 20th, 2022. See the published version at https://doi.org/10.1186/s40623-021-01545-7.

Title: Martian Moons Exploration MMX: Sample Return Mission to Phobos Elucidating Formation Processes of Habitable Planets

Author #1: *Kiyoshi Kuramoto, Hokkaido University, Sapporo, Japan/Institute of Space and Astronautical Science, Japan Aerospace Exploration Agency, Sagamihara, Japan, keikei@ep.sci.hokudai.ac.jp

Author #2: Yasuhiro Kawakatsu Institute of Space and Astronautical Science, Japan Aerospace Exploration Agency, Sagamihara, Japan, kawakatsu.yasuhiro@jaxa.jp

Author #3: Masaki Fujimoto, Institute of Space and Astronautical Science, Japan Aerospace Exploration Agency, Sagamihara, Japan, fujimoto.masaki@jaxa.jp

Author #4: Akito Araya, The University of Tokyo, Tokyo, Japan, araya@eri.u-tokyo.ac.jp

Author #5: Maria Antonietta Barucci, Laboratoire d'Etudes Spatiales et d'Instrumentation en Astrophysique, Paris Observatory, Meudon, France, antonella.barucci@obspm.fr

Author #6: Hidenori Genda, Tokyo Institute of Technology, Tokyo, Japan, genda@elsi.jp

17 Author #7: Naru Hirata, Aizu University, Aizu Wakamatsu, Japan, naru@u-aizu.ac.jp

18 Author #8: Hitoshi Ikeda, Institute of Space and Astronautical Science, Japan Aerospace

19 Exploration Agency, Sagamihara, Japan, ikeda.hitoshi@jaxa.jp

20 Author #9: Takeshi Imamura, The University of Tokyo, Tokyo, Japan,

21 t_imamura@edu.k.u-tokyo.ac.jp

22 Author #10: Jörn Helbert, Deutsches Zentrums für Luft- und Raumfahrt, Berlin,

23 Germany, Joern.Helbert@dlr.de

24 Author #11: Shingo Kameda, Rikkyo University, Tokyo, Japan, kameda@rikkyo.ac.jp

25 Author #12: Masanori Kobayashi, Chiba Institute of Technology, Narashino, Japan,

26 kobayashi.masanori@it-chiba.ac.jp

27 Author #13: Hiroki Kusano, National Institutes for Quantum and Radiological Science

28 and Technology, Chiba, Japan, kusano.hiroki@qst.go.jp

29 Author #14: David J. Lawrence, Johns Hopkins University Applied Physics Laboratory,

30 Laure, USA, David.J.Lawrence@jhuapl.edu

31 Author #15: Koji Matsumoto, National Astronomical Observatory of Japan, Mitaka,

32 Japan, koji.matsumoto@nao.ac.jp

33 Author #16: Patrick Michel, Université Côte d'azur, Observatoire de la Côte d'Azur,
34 CNRS, Laboratoire Lagrange, Nice, France, michelp@oca.eu
35 Author #17: Hideaki Miyamoto, The University of Tokyo, Tokyo, Japan, hm@sys.t.u-
36 tokyo.ac.jp
37 Author #18: Tomokatsu Morota, The University of Tokyo, Tokyo, Japan,
38 morota@eps.s.u-tokyo.ac.jp
39 Author #19: Hiromu Nakagawa, Tohoku University, Sendai, Japan,
40 hiromu.nakagawa.c1@tohoku.ac.jp
41 Author #20: Tomoki Nakamura, Tohoku University, Sendai, Japan,
42 tomoki.nakamura.a8@tohoku.ac.jp
43 Author #21: Kazunori Ogawa, Institute of Space and Astronautical Science, Japan
44 Aerospace Exploration Agency, Sagamihara, Japan, ogawa.kazunori@jaxa.jp
45 Author #22: Hisashi Otake, Institute of Space and Astronautical Science, Japan
46 Aerospace Exploration Agency, Sagamihara, Japan, ootake.hisashi@jaxa.jp
47 Author #23: Masanobu Ozaki, Institute of Space and Astronautical Science, Japan
48 Aerospace Exploration Agency, Sagamihara, Japan, ozaki.masanobu@jaxa.jp

49 Author #24: Sara Russel, Natural History Museum, London, UK,

50 sara.russell@nhm.ac.uk

51 Author #25: Sho Sasaki, Osaka University, Osaka, Japan, sasakisho@ess.sci.osaka-

52 u.ac.jp

53 Author #26: Hirotaka Sawada, Institute of Space and Astronautical Science, Japan

54 Aerospace Exploration Agency, Sagamihara, Japan, sawada.hirotaka@jaxa.jp

55 Author #27: Hiroki Senshu, Chiba Institute of Technology, Narashino, Japan,

56 senshu@perc.it-chiba.ac.jp

57 Author #28: Shogo Tachibana, The University of Tokyo, Tokyo, Japan /Institute of

58 Space and Astronautical Science, Japan Aerospace Exploration Agency, Sagamihara,

59 Japan, tachi@eps.s.u-tokyo.ac.jp

60 Author #29: Naoki Terada, Tohoku University, Sendai, Japan,

61 teradan@pat.gp.tohoku.ac.jp

62 Author #30: Stephan Ulamec, Deutsches Zentrums für Luft- und Raumfahrt, Berlin,

63 Germany, Stephan.Ulamec@dlr.de

64 Author #31: Tomohiro Usui, Institute of Space and Astronautical Science, Japan

65 Aerospace Exploration Agency, Sagamihara, Japan, usui.tomohiro@jaxa.jp

66 Author #32: Koji Wada, Chiba Institute of Technology, Narashino, Japan,

67 wada@perc.it-chiba.ac.jp

68 Author #33: Sei-ichiro Watababe, Nagoya University, Nagoya, Japan,

69 seicoro@eps.nagoya-u.ac.jp

70 Author #34: Shoichiro Yokota, Osaka University, Osaka, Japan, yokota@ess.sci.osaka-

71 u.ac.jp

72

73 *The corresponding author

74

Abstract

Martian moons exploration, MMX, is the new sample return mission planned by the Japan Aerospace Exploration Agency (JAXA) targeting the two Martian moons with a scheduled launch in 2024 and a return to the Earth in 2029. The major scientific objectives of this mission are to determine the origin of Phobos and Deimos, to elucidate the early Solar System evolution in terms of volatile delivery across the snow line to the terrestrial planets having habitable surface environments, and to explore the evolutionary processes of both moons and Mars surface environment. To achieve these objectives, during a stay in circum-Martian space over about 3 years MMX will collect samples from Phobos along with close-up observations of this inner moon and carry out multiple flybys of Deimos to make comparative observations of this outer moon. Simultaneously, successive observations of the Martian atmosphere will also be made by utilizing the advantage of quasi-equatorial spacecraft orbits along the moons' orbits.

Keywords

Phobos, Deimos, Mars, sample return mission, early solar system, habitable planet

Introduction

Amongst the numerous moons currently known in the Solar System, there are only three orbiting terrestrial planets, Phobos and Deimos being the two of them. The exploration of the Earth's Moon, which includes sample return missions, has provided us a wealth of data revealing and constraining both its formation and evolution processes and those of the parent planet. The same is probably true for the two Martian moons which also likely formed associated with the formation of their parent planet. However, the direct exploration of the Martian moons has been quite limited so far.

The Martian Moons eXploration (MMX) mission will carry out a direct, extensive survey of the Martian moons including the first sample return from one of these moons. The past explorations of the Martian moons were largely limited to flybys by orbiters approaching Mars. The first close-up imaging of Phobos and Deimos was conducted by the Viking mission, which found their irregular shapes and their albedos as low as those of asteroids thought to have carbonaceous compositions (Veverka and Duxbury 1977; Tolson et al. 1978; Pang et al. 1978; Pang et al. 1980). This led to the asteroid capture

hypothesis for the origin of both moons (Pollack et al 1979; Hunten 1979). Direct exploration of Phobos was attempted by Phobos 1 (1988), Phobos 2 (1988-1989), and Phobos-Grunt (2011), but they, unfortunately, failed except for valuable, but incomplete data acquisition by Phobos 2 in the vicinity of Phobos (Duxbury et al. 2014 for a comprehensive summary of the past explorations of Phobos and Deimos). Although several mission concepts have been proposed to explore the Martian moons, MMX is currently the only approved mission targeting the Martian moons.

For the last two decades, JAXA has been a pioneer in small body sample return missions, accumulating unique experience through the first asteroid sample return mission Hayabusa (originally named MUSES-C, 2003-2010), to the S-type asteroid Itokawa followed by the Hayabusa2 mission (2014-present) to the C-type asteroid Ryugu. Both missions have been successfully revealing how solid materials were built up to form small bodies which then migrated to near-Earth orbits involving disruption and re-accumulation processes during Solar System evolution (e.g. Fujiwara et al. 2006; Watanabe et al. 2019; Sugita et al. 2019; Michel et al. 2020). In particular, the Hayabusa2 mission is elucidating processes that may have supplied water and organics

to Earth. MMX will expand these Japanese experiences and successes in small body explorations to the Martian moons.

As a Mars orbiter, on the other hand, MMX will extend JAXA's experiences in gravitational body explorations gained by Kaguya (SELENE, 2007-2009) at the Moon and ongoing Akatsuki (Planet-C, 2010-present) at Venus. The attempted Japanese Mars orbiter Nozomi (Planet-B, 1998-2003) launched by ISAS before the institution integration into JAXA, unfortunately, resulted in contact loss during the cruise to Mars. Hence, the MMX mission is an important milestone to expand the Japanese space program to Mars synergistically with small body exploration programs.

This paper presents the current design of the MMX mission with a special focus on the scientific objectives as well as the mission requirements, the system architecture, and the observation operations plan to achieve those objectives. Note that the MMX mission is under development therefore its details may be modified in the future.

Phobos, Deimos, and Mars: Genetic and Evolutionary Links

Mars, the host planet of Phobos and Deimos, is the planet that has an atmosphere-

144 covered surface environment most analogous to that of the Earth. Abundant fluvial
145 geomorphological features such as valley networks and outflow channels strongly imply
146 the activities of a vast amount of liquid water on the Martian surface before ~3 Gya
147 (e.g. Carr 1996). Long-term volcanic activities leaving igneous provinces and volcanoes
148 may significantly contribute to volatile supply from the interior to the surface (e.g.
149 Greely, 1987). Recent precise imaging spectroscopy from orbits (e.g. Bibring et al.
150 2006) and in-situ geological surveys conducted by rovers (e.g. Grotzinger et al. 2014)
151 accumulate evidence for the widespread existence and past activities of liquid water
152 with compositions suitable for habitats. On the other hand, Mars preserves ancient
153 terrains with numerous impact craters and may be the only planet for which we can
154 precisely trace the history back to the early evolution of a hydrosphere on a rocky
155 planet. It seems, however, difficult to approach Mars formation processes through Mars
156 surface exploration alone because resurfacing processes significantly obscure records of
157 the planet formation. In contrast, the airless Martian moons with sizes too small to
158 activate long-term igneous processes likely preserve materials at their formation without
159 severe alteration, possibly providing a window to explore key processes forming Mars.
160

161 The size of Mars, which is about half of that of Earth, and the formation time of Mars
162 which is within several Myr since the start of the Solar System constrained from
163 radioisotope studies (Dauphas and Pourmand 2011) are consistent with the typical
164 characteristics of proto-planets predicted by planet formation theory (Kokubo and Ida
165 1998). Here, a proto-planet refers to the product of oligarchic growth that would have
166 occurred in a localized feeding zone of the planetesimal population. As a result of
167 oligarchic growth, the inner Solar System may have once contained dozens of proto-
168 planets with typical masses from lunar to Martian ones. Their subsequent mutual
169 collisions that occurred episodically over the time scale several 10^7 years mostly after
170 the dissipation of solar nebula gas would lead the proto-Earth and proto-Venus to
171 accumulating their current masses (Kokubo and Ida 1998). In contrast, isotopic
172 heterogeneities of extinct radionuclide systematics observed in Martian meteorites
173 suggest insufficient mantle mixing of Mars, implying the lack of complete melting
174 event possibly induced by the collision of a proto-planet (Debaille et al. 2007; Kleine et
175 al. 2009). As a fossil of proto-planet, therefore, Mars may be the unique research target
176 for revealing the processes of proto-planet formation and evolution. Inhibition of the

177 growth of Mars exceeding the present mass implies that the population of planetesimals
178 in the early Solar System rapidly declined in the region beyond the current orbital radius
179 of Mars, which might be caused by the gravitational perturbation of proto-Jupiter that
180 once migrated inward significantly (Walsh et al. 2011). This proposed mechanism may
181 have also played an important role in delivering water-bearing objects formed in the
182 outer Solar System to the terrestrial planets. The exploration of Martian moons may
183 place important constraints on such a model.
184
185 The presence of water and atmosphere is believed to be a primarily necessary condition
186 to make a rocky planet habitable. Although the origin of water and other volatiles on the
187 terrestrial planets remains controversial, one of the dominant hypotheses is the delivery
188 by late accreting bodies originated in the outer Solar System (Genda 2016 for review).
189 This is because the rocky planets are thought to be born dry if they were made from
190 solid materials accreted in the inner solar nebula where nebular gas was too warm for
191 water vapor to condense onto dust. In the outer solar nebula, beyond the snow line,
192 water may condense as ice, which allows the formation of icy planetesimals. A part of
193 them may further evolve and migrate to become rocky asteroids in the asteroid belt (e.g.

194 Walsh et al. 2011), containing hydrated minerals generated through the chemical
195 reactions of silicates with liquid water produced by internal heating (e.g. Fujiya et al.
196 2012). Observed compositions of meteorites and comets suggest that such hydrated and
197 icy bodies are also enriched in carbon and nitrogen mainly in the form of complex
198 organic matter (e.g. Kallemeyn and Wasson 1981; Mumma and Charnley 2011). Mars is
199 in the best position to elucidate how such volatile-rich bodies are transported in the
200 early Solar System because it is the terrestrial planet orbiting nearest the snow line.
201
202 Compared to the Earth's Moon, Phobos and Deimos are characterized by their smallness
203 in size, low bulk densities, irregular shapes, and very low albedos (Table 1). They share
204 visible to near-infrared reflectance spectra with reddening trends like those of D-type
205 and T-type asteroids which are thought to have volatile-rich, carbonaceous compositions
206 (Rivkin et al. 2002). Their small sizes and low bulk densities appear to be within the
207 range of undifferentiated small bodies (e.g. Burns 1978). According to the spectroscopic
208 classification of asteroids, the above types of asteroids are likely originated in the region
209 near the Jovian orbit (DeMeo and Carry 2014). These facts naturally lead to the capture
210 hypothesis for the origin of the Martian moons; carbonaceous primitive bodies

211 originally formed beyond the snow line of the Solar System might have migrated
212 inward (Walsh et al. 2011) and then become captured by Mars. If this is the case, the
213 exploration of Martian moons will provide us clues for the delivery processes of water
214 and other volatiles from the outer Solar System to early terrestrial planets.
215 (Table 1)
216
217 The feasibility of asteroid capture to form the Martian moons is, however, controversial.
218 To capture a heliocentric body as a satellite, dissipation of orbital energy relative to the
219 planet is required. Models of aerodynamic capture have suggested that heliocentric
220 bodies with sizes similar to Phobos and Deimos are possibly captured by proto-Mars
221 embedded in the solar nebula gas (Hunten 1979; Pollack et al. 1979). The orbit of a
222 captured body gradually circularizes and then decays toward a collision with the
223 planetary surface. Thus, the aerodynamic capture scenario requires some mechanism to
224 terminate the action of aerodynamic drag, such as the loss of an extended atmosphere
225 containing a small number of capture bodies (Hunten 1979). On the other hand, Phobos
226 and Deimos have low orbital inclinations and eccentricities (Table 1). Since heliocentric

227 bodies that encounter a planet may approach from almost random directions, the
228 resulting orbital inclinations of captured bodies are likely also random relative to the
229 planetary equatorial plane as seen in irregular satellites of giant planets. Tidal
230 interactions with Mars seem too weak to reduce the orbital inclinations of captured
231 bodies during its history given initial large inclinations (Rosenblatt 2011). An
232 alternative mechanism to reduce inclination may be gas-drag in a proto-atmosphere or
233 circum-planetary gas envelope rotated in the same direction of the planetary rotation. It
234 remains, however, poorly understood how such atmospheric conditions may be
235 established and effectively work to produce moons with near-equatorial orbits.
236
237 The giant impact origin hypothesis, the other leading theory for the formation of the
238 Martian moons, could satisfy the constraints from their orbits. Tidal interactions with
239 Mars make Phobos orbit decline and Deimos one expand. Hence, their original orbits
240 would be near the co-rotation radius of Mars located at a distance of ~6 Martian radii
241 from the planetary center (Burns 1978). Recent dynamical simulations of impact ejecta
242 released from huge (potential) impact structures with a scale comparable to the Borealis

basin, for example, succeed to explain small masses and near-circular equatorial orbits of both moons (Rosenblatt et al. 2016; Canup and Salmon 2018). To reconcile with the formation of moons near the co-rotation radius, the total mass of impact ejecta extended to several Martian radii should be much larger than that of both moons, thereby leading to the formation of an inner large moon through the accretion of ejecta materials. Such a large moon may gravitationally excite the random motion of debris in the outer ejecta disk and promote their collisional coagulation into a small number of tiny moons. The inner large moon would eventually fall onto Mars due to tidal interactions leaving the two tiny moons with near-circular and near-equatorial orbits in the vicinity of the co-rotation radius of Mars. In an extended giant impact origin scenario, Phobos may be the youngest generation of the inner moon that has repeated tidal break-ups, followed by orbital diffusion of disrupted debris and their partial re-accumulation during the secular tidal orbital evolution (Hesselbrock and Minton, 2017). Note, however, that clear geologic evidence has been yet unidentified for the mass loss of large inner moon onto the Martian surface so far.

An elaborate numerical analysis of the giant impact model for the origin of the Martian moons predicts that the Martian moons consist of a near 50:50 mixture of impactor materials and proto-Mars materials (Hyodo et al. 2017). If this is the case, the Martian moons will provide us clues for the composition of both the impactor and the proto-Mars, which will also allow improving drastically our understanding of the giant impact phenomena that resulted in the formation of both moons. For instance, high energy density gained from the giant impact process likely left igneous mineralogy and texture for the Martian moon materials. On the other hand, it remains unclear how such materials lead to the current reflectance spectra of Phobos and Deimos.

Altogether, the origin of the Martian moons is still controversial to date. The current pros and cons of the two major hypotheses of the Martian moon origin are summarized in Table 2. Of course, one cannot rule out alternative scenarios such as the co-accretion of moons around a growing Mars. If MMX results lead to an alternative scenario for the origin of Martian moons, unexpected new aspects will be revealed not only for both moons but also for the formation of Mars.

(Table2)

Phobos, Deimos, and their surrounding space are also expected to contain clues to understand the evolutionary processes not only on both moons but also on Mars, such as impact flux to the Mars-moons system, resurfacing of satellite surfaces by meteoroid impacts, contamination of impact ejecta from Mars onto the moons' surface, the outflow of the Martian atmosphere, implantation of particles originated from solar wind and Martian atmosphere, possible gas emission from the interiors of the moons, possible formation of dust ring or torus along the moons orbits, and tidal deformation. These are valuable processes to be explored by missions to the Martian moons. Also, from the space around the near-equatorial orbits of the Martian moons, a spacecraft can make monitoring observations of the Martian atmosphere by taking successive images and spectra covering the wide-area of the planet's hemisphere. Such observations are complementary to the low altitude, close-up observations conducted by the previous Mars orbiters.

Mission Objectives and Requirements

Mission objectives

To reveal the origin of the Martian moons and elucidate the evolution of Mars and the habitable terrestrial planets in the Solar System, the MMX mission has selected Phobos as the target for sampling and thus for detailed observations. Of course, it would be ideal to take samples from both moons, but this is infeasible because of the limitation of mission resources. The reasons for choosing Phobos as the sampling target are as follows: First, the surface of Phobos exhibits a larger spectral diversity than Deimos (Rivkin et al. 2002; Fraeman et al. 2014). This implies that the composition of Deimos may be within the range of compositional diversity of Phobos material. Note that spectral diversity might also reflect differences in physical states such as grain size distribution of surface regolith rather than compositional difference. Second, Phobos' surface likely contains a certain amount of materials ejected from young impact craters on Mars (Ramsley and Head 2013; Hyodo et al. 2019), which might provide us information on the past surface environment of Mars at the time of bedrock formation before cratering (Usui et al. 2019). Third, more abundant imaging data have been accumulated for Phobos, which allows us to optimize the landing strategies and

operations before the launch of the spacecraft.

Referring to the advantage offered by the Martian moons for elucidating processes producing habitable terrestrial planets, the MMX mission places scientific objectives as listed in Table 3, where the major goals and medium objectives flow down to the specific objectives and mission requirements. The two major goals are to elucidate the origin of terrestrial planets with habitable environments and to identify and characterize important evolutionary processes of the Mars system consisting of Mars, its moons, and the circum-Martian space. As for the former goal, the MMX mission aims first to reveal the origin of the Martian moons (medium objective 1.1). Either of the medium objectives 1.2a or 1.2b become activated depending on the actual origin of Phobos. If the moons are found to be of capture origin, then the formation and dynamical transport of original bodies will be deciphered along with their cosmochemical characteristics through sample analyses (1.2a). If they are found to be of giant impact origin, then the timing and magnitude of the impact will be estimated along with the composition of the impactor, which is indicative of its formation region, by sample analyses (1.2b). As for

the Mars system evolution, MMX will reveal alteration processes of surface layers of Phobos and Deimos (2.1), take new constraints on the Martian surface environment evolution (2.2) and characterize the dynamical behavior of the Martian atmosphere that relates to the atmospheric evolutionary processes (2.3). Processes such as possible dust and/or gas torus formation along orbits and supply of Mars-derived rocky materials onto Phobos may be unique for the Mars system.

(Table 3)

Considering that the MMX mission has been assembled from the primary objective of exploring the Martian moons, the mission objectives are prioritized as shown by the marks in Table 3. Determination of the origin of Phobos by spectroscopic observations (MO1.1.1) and by sample analyses (MO1.1.2) has the highest priority as well as the identification of weathering and evolutionary processes of Phobos surface (MO2.1.1). Constraining Phobos' origin from its molecular release rate, mass distribution, and surface density variation (MO1.1.3) is given high priority as well as revealing the surface distribution of constituent materials in Deimos in comparison with those of

Phobos (MO1.3.1). The second priority is also given for constraining the initial conditions of celestial migration processes and evolution of the Martian surface from predictions of the capture process (MO1.2a.1), and estimating the magnitude and timing of the giant impact along with placing constraints for celestial migration and planetary formation processes (MO1.2b.1). Objectives related to the observations of the Martian atmosphere (MO2.2.2 and MO2.3.1) and the possible finding of particles ejected by impact cratering on Mars since the formation of Phobos (MO2.2.1) are given third priority.

Mission requirements

Corresponding to each mission objective, the mission requirements are deduced by reflecting the current knowledge of the Martian moons and their parent planet (Table 3). The detailed requirements concerning resolutions and accuracies for each type of observation will be given by corresponding instrument papers. The general scientific grounds for each mission requirement are described below.

MR1.1.1 summarizes the requirements for remote sensing observations to constrain the origin of Phobos. Previously obtained visible and near-infrared reflectance spectra of Phobos are almost featureless with possible weak features indicative of olivine and pyroxene (Gendrin et al. 2005) and phyllosilicates (Fraemann et al. 2014) but there remain the limitation of S/N, spatial resolution, and/or coverage. If hydrated minerals are proven to exist in fresh bedrock exposures, this provides strong evidence for the capture origin of Phobos. Since the Phobos surface is possibly affected by space weathering and late accumulated materials, it is valuable to determine reflectance spectra for fresh materials exposed in and around young craters with diameters of about 100 m or larger. To achieve such observations, a spatial resolution of 20 m or better is required for spectroscopic mapping of major areas on Phobos. High spatial resolution is also valuable to determine the reflectance spectra of tens-m-size boulders which may contain freshly exposed surfaces. Imaging with a spatial resolution of 1 m or better is necessary for ~50 m area including sampling site to characterize the geologic context of samples. The mean Si/Fe ratio on the hemisphere scale, which is observable by a

372 gamma-ray spectrometer for instance, also provides an important clue to revealing
373 Phobos origin. If capture origin is the case, Si/Fe ratio is expected to be within the range
374 of chondritic meteorites. If the giant impact origin is the case, Si/Fe ratio may be > 20%
375 larger than the chondritic range (1.1-2.0 Wasson and Kallemeyn 1988) due to the
376 contribution of Mars mantle materials.
377
378 MR1.1.2 describes the mission requirement for sampling and sample analyses to
379 determine Phobos' origin. To collect Phobos indigenous materials from the surface
380 possibly contaminated by exogenic materials, a large amount of granular sample is
381 necessary for statistical sorting by the isotopic composition. The average mixing ratio of
382 external materials is estimated to be several % at most (Ramsley and Head 2013; Hyodo
383 et al. 2019). To distinct possible chemical diversity in indigenous materials and external
384 materials by statistical analyses, at least about one hundred particles with size applicable
385 for isotopic composition determination are necessary. The typical size of Phobos
386 regolith particles is estimated to range from 300 μm to 2 mm (see section “Sampling
387 and Sample Analyses”). 300 μm is enough for three oxygen isotope determination and

388 ~1 mm is enough for $^{53}Cr/^{54}Cr$ determination with sufficient accuracy (Usui et al. 2020).
389 Both isotope systems provide a key proxy to judge the type of the source body (Warren,
390 2011). Of course, complimentary application of textural, mineralogical, and chemical
391 analyses for grains is also useful to judge the origin of Phobos. This requires the sample
392 collection of $\geq$10 g samples for each sampling site. To obtain materials minimally
393 affected by space weathering caused by solar wind and meteoroid fluxes, samples
394 should include materials from a depth of > 2 cm that is deeper than the penetration
395 depth of solar wind (Nishiizumi et al. 2009). On the other hand, Phobos indigenous
396 materials may have compositional diversity as implied from the observed regional
397 difference in reflectance spectra represented by red unit and blue one (Rivkin et al.
398 2002; Fraeman et al. 2014). Here blue unit stands for areas having weaker reddening
399 trends, which may represent diversity in composition or weathering state on Phobos.
400 Therefore, samplings from at least two different sites are ideal. Also, to guarantee the
401 collected samples to be Phobos indigenous materials, material distribution on the entire
402 globe of Phobos as well as the geologic context of sampling sites should be constrained
403 by imaging and spectroscopic mapping.

404

405 Mission requirements for the acquisition of data related to Phobos's internal structure
406 that independently provide constraints on Phobos origin are summarized in MR1.1.3.
407 The low density of Phobos compared to intact rocks possibly reflects the existence of
408 water ice in the deep interior or a significant porosity in this moon at all depths.
409 According to the thermal evolution model of Phobos (Fanale and Salvail 1990), the
410 emanation of water molecules may continue at present depending on the thermal and
411 molecular conductivities and assuming that Phobos was originally a primitive small
412 body bearing water ice. 10^{22} molecules/s is a possible emanation rate at present. The
413 emanation of H_2O molecules, if detected, will strongly support the capture of an ice-
414 bearing small body for as Phobos' origin. The icy Phobos model also implies a
415 combination of a dense core made of a silicate-ice mixture and a porous silicate mantle
416 under the evaporative loss of ice from the surface. If mass concentration toward the
417 center is found from geodetic observation, it places important constraints on such a
418 model.

419

Depending on the revealed origin of Phobos, the mission requirements MR1.2a and MR1.2b mainly for sample analyses are given, respectively. If capture origin is the case (MR1.2a), chemical, mineralogical and isotopic compositions are required to identify the source region of the Phobos precursor. The application of chronological analyses in combination with the geological survey is required for the estimation of time and environment of the formation of the precursor body as well as for constraining the impact history during the migration in the early Solar System. Volatile abundances in Phobos indigenous materials are also necessary to evaluate how Phobos-like bodies may contribute to built-up an ancient atmosphere-ocean-cryosphere system on proto-Mars.

If giant impact origin is the case (MR1.2b), determination of textures, chemical, mineralogical and isotopic compositions, and alteration ages of Phobos indigenous materials are necessary for the estimation of the timing and magnitude of the impact event, the chemical type of the impactor, as well as the mixing ratio of materials derived from the impactor and proto-Martian mantle. To estimate the mixing ratio of the bulk

436 moon fairly extending the sample constraints, measurement of elemental ratio such as
437 Fe/Si is necessary for the Phobos surface material averaged over the hemisphere scale.
438
439 Mission requirements for constraining the origin of Deimos are described by MR1.3.1.
440 As for Deimos' observation, it is most important to confirm whether the genetic
441 commonality of Deimos and Phobos implied from the similar reflectance spectra at the
442 coarse spatial resolutions is the true character or surficial one. To achieve this, it is
443 necessary to obtain spectroscopic data constraining composition for major areas
444 containing widespread exposures of bedrocks of Deimos. A candidate area enriched in
445 such exposure is the Deimos’s south pole basin, which is possibly the largest crater on
446 Deimos comparable to the Stickney crater of Phobos. However, the topography of this
447 basin has been poorly determined so far due to the lack of image at good illumination
448 conditions (Thomas 1993). A detailed study of the topography of this basin is necessary
449 also for the estimation of the Deimos’s volume and thus density as well as for the
450 geological comparison of Deimos with Phobos.
451

452 The mission requirements given by MR2.1 are specified for clarifying the surface
453 evolution and its processes of Phobos, paying attention to the difference in boundary
454 conditions from heliocentric small bodies. Since the Martian moons revolve around
455 Mars with relatively short periods, whenever an impact occurs, a considerable fraction
456 of ejecta particles that once escape the moons' gravity may re-impact onto the original
457 moon after revolutions around Mars. Such ejecta behavior may promote the thickening
458 of regolith layers of the moons (Ramsley and Head 2013) and cause the formation of
459 dust rings (or torus) along the satellite orbit through impact ejecta reproduction (Soter
460 1971). Since Phobos is positioned slightly outside the tidal break-up radius of Mars, it
461 may experience cratering events strongly influenced by the action of Martian tidal
462 forces and/or by ejecta from Martian craters (e.g. Basilevsky et al. 2014). The tidally
463 locked rotation may induce heterogeneous evolution of the surface layer between
464 leading and trailing hemispheres due to the different flux and approaching velocities of
465 impactors (Christou 2014). The molecular flux from the Martian atmosphere may affect
466 space weathering of the moons' surface along with the influx of solar wind and
467 meteoroids (e.g., Stofer 1971; Poppe and Curry 2014). To unravel those complex

468 processes, it is necessary to conduct observations of dust and ion fluxes in circum-
469 Martian space, topography mapping with resolution enough for precise crater
470 chronology among major terrains and geomorphic features, and sample analyses
471 characterizing space weathering processes.
472
473 The mission requirements for the search for materials transferred from Mars after
474 Phobos formation in the returned sample are given by MR2.2.1. Based on the young
475 crater population on Mars and numerical simulations of impact processes, it is estimated
476 that Phobos regolith may contain on average at least 340 ppm of ejecta materials from
477 Mars due to impacts during the last 500 Myr (Hyodo et al. 2019). The contaminated
478 ejecta materials likely consist not only of igneous rocks but also of sedimentary ones.
479 10 g of granular Phobos sample may contain several tens grains of such Martian ejecta
480 assuming that 300 μm grains dominate the sample mass. Grain samples originated from
481 Martian terrains excavated by young impacts may allow material studies to characterize
482 the Martian surface environment at ages of terrain formation on Mars. To do so, it is
483 necessary to seek out impact ejecta materials from the returned samples and add

484 adequate analyses to constrain ages and deposition environments on Mars.

485

486 The mission requirement given by MR2.2.2 is placed to conduct flux measurements of
487 major escaping ion species such as O^+ and C^+ with discriminating isotopes to improve
488 constraints on the isotopic fractionation in ion escape processes. Atmospheric escape is
489 one of the significant ongoing processes at Mars that have driven the evolution of the
490 Martian surface environment over a geologic time scale (e.g. Jakosky et al. 1994). The
491 isotopic fractionation of escaping species changes the residue volatile element isotope
492 values over geological time. Thus, the isotopic fractionation factor at escape is an
493 important parameter to interpret the isotopic difference among Martian volatile
494 reservoirs in terms of the time scale and magnitude of atmospheric loss. Past Martian
495 missions and ground-based observations have progressively revealed the isotopic
496 composition of volatile elements in the Martian atmosphere and sedimentary materials
497 along with analyses of Martian meteorites (e.g. Leshin et al. 2013; Mahaffy et al. 2013;
498 Villanueva et al. 2015, Jakosky et al. 2018). However, isotopic fractionation of escaping
499 elements, which probably depends on the level of solar activity, has been poorly

500 constrained by previous studies especially for ion species (Chassefière and Leblanc
501 2004).
502
503 The mission requirement given by MR2.3 is placed to realize monitoring atmospheric
504 flow and the transport of water and dust using the vantage of the equatorial orbit
505 moderately distant from Mars. The Martian atmosphere exhibits various meteorological
506 activities. Among them, atmospheric transport of water vapor and dust plays a
507 particularly important role in the evolution of the Martian climate system. The lateral
508 water transport is an elementary process for global-scale redistribution of water storage
509 of near-surface layer over the time scale of changes in obliquity and orbital parameters
510 such as eccentricity and the argument of periapsis caused by gravitational perturbations
511 by other planets (e.g. Mastard et al. 2001). Dust that distributes everywhere in the
512 Martian atmosphere with variable content significantly influences the radiative budget
513 of the thin atmosphere since dust is the primary absorber for visible and infrared
514 radiation (Pollack et al. 1979b). Therefore, dust strongly affects the atmospheric thermal
515 budget and dynamics, which in turn influence water vapor transport, including one

across the vertical direction reaching the upper atmosphere where photolysis of water molecules takes place (e.g. Heavens et al. 2018). However, it remains poorly constrained how the dust transport is coupled with atmospheric dynamics due to the paucity of continuous imaging observations that can capture developments of dust events.

Spacecraft and Science Instruments

Spacecraft

Since the design of the MMX spacecraft architecture is reported in detail elsewhere (Kawakatsu et al. 2019), here we briefly summarize its essence. The MMX spacecraft will employ a chemical propulsion system with a high acceleration ability to confine the roundtrip time to a reasonable length (Campagnola et al. 2018). To achieve a round trip to the Martian sphere of gravity, the spacecraft is composed of separable modules: propulsion module, exploration module, and return module (Figure 1). By releasing used modules at appropriate epochs, the spacecraft mass will be reduced to allow orbital controls in the Martian system and return cruise to the Earth reducing the required

532 overall propellant mass. To carry samples with a volume much larger than that of
533 Hayabusa2 which aims to take 100 mg of samples (Tsuda et al. 2013), an enlarged
534 return capsule will be used for MMX. The total spacecraft wet mass at launch is about
535 4,000 kg. The spacecraft will be launched by an H-III rocket with launch capabilities
536 larger than H-II rockets. The H-III rocket system is under development as the new
537 Japanese flagship launch vehicle with the planned first launch in 2021.
538 (Figure 1)
539

540 ## Science instruments

541 Table 4 lists the science instruments aboard MMX. These are selected to satisfy the
542 mission requirements complimentary to the sample analyses. As the detailed description
543 of each instrument will be given elsewhere, here we summarize their complementary
544 roles.
545 (Table 4)
546

547 One of the most important roles of proximity observations is to obtain constraints for

548 the origin of the Martian moons independently of sample analyses and also to document
549 the sampling site to inform the geological context. Measurements for the determination
550 of bulk Phobos composition is the most direct approach for this purpose. OROCHI
551 (Kameda et al. this issue), the wide-angle visible multiband camera, and MIRS (Barucci
552 et al. this issue.), the infrared spectrometer, will conduct near-global mapping of
553 reflectance spectra of Phobos with spatial resolutions of the order of 10 meters.
554 Combining with the specification of fresh surface exposures by TENGOO (Kameda et
555 al. this issue), a panchromatic telescopic camera with much higher spatial resolutions,
556 the spectroscopic mapping over wavelength from visible to infrared will constrain the
557 mineral composition of Phobos bedrock. Hydrous minerals are a very important proxy
558 indicative of the captured origin of the moon, thus OROCHI and MIRS are designed to
559 detect absorption bands at ~0.7 μm and ~2.7 μm, respectively, caused by hydroxyl
560 group in mineral structures with sufficient signal to noise ratio.
561
562 MEGANE (Lawrence et al. 2019), the gamma-ray and neutron spectrometer will
563 determine the concentration of elements such as Si, Fe, H, and K in the surface layer of

564 several tens cm thickness, where cosmic-ray induced and spontaneous atomic nucleus
565 reactions take place associated with emissions of neutrons and high energy photons to
566 space, over the hemisphere scale. MSA (Yokota et al. this issue.), the ion mass spectrum
567 analyzer, will attempt to detect the ion torus derived from H_2O possibly released from
568 Phobos which may store icy materials inside. Metallic ions spattered out from the
569 surface of Phobos by solar wind are also the target of the MSA measurements, which
570 may constrain the elemental composition of Phobos surface averaged over the
571 hemisphere scale as is the case for the Earth`s moon (Yokota et al. 2009).
572
573 LIDAR (Senshu et al. this issue), the laser altimeter, will be used for the determination
574 of the shape, rotation, and gravity field of Phobos in combination with the topographic
575 imaging by TENGOO and Earth-based spacecraft tracking data. Combining the
576 rotational quantity with the gravity field determination based on precise analyses of
577 inertial spacecraft motion around Phobos, one can deduce constraints on Phobos's
578 internal density distribution such as the moment of inertia factor. A shape model
579 provides the position of the center of mass relative to the geometrical center. These may

580 reflect possible compositional heterogeneity of this moon, for instance, the presence of
581 interstitial ice in the deep interior, the presence of porosity, or the coalescence of
582 planetesimals with different compositions. LIDAR will also provide surface roughness
583 information within each laser footprint from analysis of the reflectance as a function of
584 observation angle at the laser wavelength of 1064 nm.
585
586 Those remote sensing data will be also used for the selection of sampling sites that are
587 required to be sufficiently flat for safe landing and accessibility to Phobos indigenous
588 materials. The global surface composition of Phobos constrained by proximity
589 observations will be compared with the compositions of the returned sample to examine
590 how returned materials are representative of Phobos indigenous materials. Close-up
591 spectroscopic and panchromatic imaging by OROCHI and TENGOO with spatial
592 resolutions in the order of mm during landing operations will be used to describe the
593 geologic context of the sampling site, which is necessary to interpret the possible
594 variation of composition and grain size, texture, and weathering state of returned
595 samples.

596

597 The topographic and compositional mapping data will be also used to elucidate the
598 geologic processes that have evolved the surface of Phobos in the areocentric orbit.
599 Crater counting with higher spatial resolution provides a basis for its resurfacing
600 history. CMDM (Kobayashi et al. 2018) is a dust detector monitoring impact signals on
601 its sensor of an exposed thin film at the top layer of multi-layer insulation of the
602 spacecraft. It will measure the impact momentum of dust particles colliding with the
603 sensor surface in orbit around Mars. When there is a dust collision on the sensor, it is
604 classified as interplanetary dust, interstellar dust, or Mars orbiting dust based on the
605 information on the orbital position and attitude of the spacecraft at that time. As a result,
606 the flux of those dust species is obtained. Confirmation of the presence or absence of a
607 hypothesized dust ring or torus along the moons' orbits is one of the main purposes of
608 this measurement. Furthermore, the measured fluxes of dust particles including
609 meteoroids provide basic data for understanding the weathering and impact gardening
610 processes of both moons. By combining the analyses of samples concerning impact
611 alteration states and ages, mixing of exotic materials, and possible material exchange

among bodies in the Martian system, an integrated view for the surface evolution of the Martian moons would be available.

OROCHI and MIRS will also conduct a series of spectroscopic imaging/mapping of the atmosphere of Mars. From positions near Phobos, both instruments are capable of imaging a wide area from mid to low latitudes of Mars. At positions more distant from Mars, imaging of the global hemisphere becomes easier. Color imaging by OROCHI can identify ice clouds and atmospheric dust, whereas infrared spectroscopic imaging by MIRS can assess the distribution of the column H_2O vapor content using the reflectance contrast between the wavelengths in and outside the H_2O absorption band. By tracing the motion of clouds, atmospheric dust swarms, and H_2O vapor using the time series of imaging/spectroscopic data, the atmospheric circulation can be understood and the exchange of H_2O among the surface reservoirs can be constrained. Additionally, zoom-up observations by TENGOO would capture the upwelling of dusty warm air into the upper atmosphere, which may be a key process promoting H_2O photolysis and H escape to space (Heavens et al. 2018). Ions escaping from the Martian

628 upper atmosphere are detectable by MSA with distinguishing isotopic mass of elements
629 including O and C. This would provide us better constraints on isotopic fractionation in
630 the atmospheric escape processes. From those observations of the Mars atmosphere, one
631 can reveal atmospheric processes that have driven the evolution of the Martian surface
632 environment.
633
634 MMX will carry a rover provided by CNES and DLR for scientific and engineering
635 purposes including being a scout for the lander (Michel et al. this issue). The landing
636 system and landing operation of the mothership have been studied to absorb the
637 uncertainties in the mechanical properties of Phobos surface regolith such as the surface
638 layer strength. On the other hand, it is beneficial to confirm in advance whether the
639 actual regolith properties are within or outside the expected range. The rover will be
640 released before the landing operation and conduct an in-situ examination of the Phobos
641 surface. The rover powered by its solar generator will be equipped with navigation
642 cameras, wheels for travel with torque sensors, wheel cameras, imaging the interaction
643 of the wheels with the regolith, a thermal radiation monitor (MiniRad), accelerometers

644 characterizing impact and bouncing, and a laser Raman microscope, RAX (Cho et al.
645 this issue). These instruments will examine mechanical, dynamical, and thermal
646 properties and mineralogy of Phobos surface regolith. The obtained data are also useful
647 as ground truth for interpreting the remote sensing data taken from orbit.
648
649 The sampling system, one of the most important mission instruments of MMX, will
650 conduct sampling from Phobos surface regolith and transfer of samples into a sample
651 container inside the sample return capsule (Kawakatsu et al. 2019). After touch down,
652 sampling will be conducted by using a joint arm manipulator equipped with a coring
653 mechanism at its tip. The MMX mission is planned to make landings at two different
654 sites. At each landing site, a sampling point will be first determined within the area
655 accessible by manipulation based on a precise raw surface image transmitted to the
656 ground station on Earth. An installed corer with an inner diameter of 2 cm will penetrate
657 to a sufficient depth at the designated point and then the inner sample holder will be
658 transferred to the container space in the return capsule. OROCHI will conduct
659 spectroscopic imaging of the sampling point and its surroundings with a spatial

660 resolution of the order of mm to specify their spectroscopic property and geologic
661 context which are important to assess how the acquired samples are representative of
662 Phobos indigenous materials.
663
664 A pneumatic sampler, another type of sampler provided by NASA applying the same
665 working principle as used during the OSIRIS-Rex mission (Bierhaus et al. 2018),
666 installed at a landing pad will also attempt sampling of regolith at shallow depth
667 (Kawakatsu et al. 2019). Samples taken from different depths are useful to understand
668 the possible layering of surface regolith caused by space weathering, the influx of exotic
669 materials, and gardening by meteoroid impacts (Usui et al. 2020). We call this sampler
670 P-sampler whereas the primary coring sampler is called C-sampler. The sample holder
671 of the P-sampler will be transported to the container space in the return capsule by the
672 manipulator.
673

674 # Mission Profile

675 ## Overall

676 The planned mission profile is shown in Figure 2. The MMX spacecraft is planned to be
677 launched in September 2024 and reach the Martian system after the cruise slightly less
678 than a year. The spacecraft will stay in the Martian system for nearly 3 years and
679 conduct close-up observations of both moons, delivery of the rover, and sampling from
680 Phobos. The spacecraft will depart the Martian system in August 2028 and return the
681 capsule containing collected samples to the Earth.
682 (Figure 2)
683
684 After the insertion to a circum-Martian orbit, the spacecraft motion will be tuned to
685 approximate the Phobos motion. By taking small differences in orbital eccentricity from
686 Phobos, the spacecraft will eventually circulate Phobos at small distances. In the frame
687 fixed to Phobos, the spacecraft trajectory will form an ellipse, or quasi-satellite-orbit
688 (QSO), with the center at the Phobos mass center (Figure 3). The semimajor axis of
689 QSO, which is perpendicular to the Mars direction, is about twice of the minor axis.
690 Decreasing in separation from Phobos, QSO gradually approaches to circle, or the
691 semimajor axis/minor axis ratio decreases, due to the greater contribution of Phobos

692 gravity. MMX will utilize several QSO patterns with high (semimajor axis 200 km,
693 QSO-H), medium (100 km, QSO-M), and low (50 km and below, QSO-L series)
694 altitudes depending on the observation phase. MMX will also introduce the so-called
695 3D-QSO with inclination to Phobos, which allows observation of high latitude regions
696 of this moon (Figure 3b). From QSOs, MMX will carry out observations of Phobos
697 including those for landing site selection, circum-Martian space, and the Martian
698 atmosphere.
699 (Figure 3)
700
701 During the period in proximity to Phobos, the spacecraft will land on two different sites
702 of Phobos. Since Phobos's surface gravity is two orders of magnitude larger than those
703 of Itokawa and Ryugu, the descent and landing sequence of MMX spacecraft is
704 different from the prior missions Hayabusa and Hayabusa2 which used a so-called
705 touch and go approach for sampling operations. For example, a low-velocity descent
706 from a very high altitude cannot be adopted considering fuel consumption to keep low
707 velocity against gravity. Instead, from low QSO orbit, a ballistic descent will be applied

to reach ~2 km above a landing site before starting the subsequent final vertical descent. A rehearsal operation before landing will take close-up images of the area including landing site candidates to confirm the safety and the availability of samples that are representative of bedrock materials. To avoid previously unrecognized obstacles such as large boulders in the area of the selected site, an autonomous hazard detection and avoidance technology will also be set up to realize a safe landing. The landing gear is installed with a mechanism absorbing the spacecraft momentum relative to the surface to prevent the spacecraft from bouncing at touch down.

After the completion of proximity observations of Phobos and sampling operations, the spacecraft will expand its orbit to perform multiple flybys of Deimos. During this period, close-up observations of Deimos will be conducted together with those of the surrounding space and the Martian atmosphere. Then, the spacecraft will depart from the Martian system.

Operations during the stay around the Martian moons

In the nominal operation plan, solar conjunctions will occur in January 2026 and March 2028 during the stay around Mars. Science operations may be inhibited for ~1.5 months around these conjunction timings. Furthermore, Mars will arrive at equinoxes in late November 2025 and this will happen subsequently after every about half of the Martian year. During about three months with each conjunction timing in the middle, low QSOs around Phobos will experience eclipses with long duration by Mars and Phobos repeatedly. This is caused by the near-equatorial orbit of Phobos around Mars and relatively small differences in QSO periods from the length of the day of Phobos. For maintaining the health of electric devices, long stops of power generation should be avoided. During those periods around equinoxes, therefore, QSO operation is restricted to large ecliptic orbit with minor and major radii no smaller than 50 km and 100 km around Phobos to reduce the duration of every eclipse.

The current plan for observational operation is shown in detail elsewhere (Nakamura et al. this issue), here we briefly overview it below. Considering the constraints shown

740 above, the period of ~3 years stay in the sphere of Martian gravity is divided into five
741 phases as shown in Figure 4. Period 1 starts from MOI (Mars Orbit Insertion). After
742 MOI, the spacecraft will be transferred to QSO around Phobos after the deployment of
743 the propulsion module. During this transfer, the spacecraft will have a chance to
744 approach Deimos at outer orbit, which would be used as an opportunity for the first
745 Deimos imaging observation from small distances. After insertion to QSO, observations
746 of Phobos from QSO with larger orbital radii (QSO-H) will be conducted for the near-
747 global shape model generation and spectral mapping of Phobos with a typical spatial
748 resolution of several meters for telescopic monochrome imaging and several 100 meters
749 for spectroscopic imaging by OROCHI and MIRS. At this time, the LIDAR footprint
750 will be several 10 m from QSO-H.
751
752 During phase 2 that starts after the first solar conjunction, close-up observations from
753 QSOs with minor and major radii as small as 30 km and 50 km or even below will be
754 combined to conduct higher resolution imaging and spectral mapping up to typical
755 spatial resolution ~40 cm and ~20 m, respectively. The LIDAR footprint will become as

small as several m. Observations from QSO with low radii are mandatory for the gamma-ray and neutron spectrometry by MEGANE which needs a large solid angle of the targeting body in the field of view to reduce sufficiently the effect of background noise.

The descent and landing operations will be performed during phase 3 using the advantage in solar illumination conditions and short Earth-Mars distance. The release of the rover and the descent and ascent operation, which is a part of the landing rehearsal, will be done before the first actual landing but their best timings are under study including the last part of phase 2. Observations with progressive improvement of spatial resolution during phases 1 and 2 will be used for the landing site selection to guarantee the safety for landing and the accessibility to indigenous materials. MMX plans to perform sampling from multiple landing sites because Phobos is known to have a composite surface made of units with colors distinguished by slopes of reflectance spectra as mentioned above.

772 A landing operation that includes touch-down, sampling, and departure will be
773 completed during a single daytime of Phobos lasting 3 hours 50 minutes. The stay time
774 on the surface is planned to be 2.5 hours with about a 1-hour margin in the entire
775 daytime. The time duration allocated for the sampling operation is 1.5 hours, which
776 includes close-up imaging of the landing area to determine the sampling point by the C-
777 sampler and the telemetries of image data and command with the control station on the
778 Earth. During the first landing, the P-sampler system whose nozzle is equipped on a
779 landing pad will be used.
780

781 ## Sample Sciences

782

783 Due to the current lack of direct measurement, the grain size distribution of Phobos
784 regolith remains uncertain. According to the interpretation of Phobos thermal inertia
785 from the modeling of thermal conduction through granular layers, the typical grain size
786 in Phobos regolith is estimated to be ~1 mm (Gundlach and Blum 2013). An expanded
787 method incorporating the physical relationships between porosity and grain size under

788 the action of intra-grain cohesion forces and Phobos's gravity suggests the typical size
789 of ~ 2 mm (Kiuchi and Nakamura 2014). Among ejecta released from the Phobos
790 surface by impacts, grains smaller than ~300 μm would be preferentially lost to the
791 parent planet or outer space due to the action of solar radiation pressure (Ramsley and
792 Head 2013) while large grains may return onto the surface of Phobos after areocentric
793 motion. For those reasons, the regolith grains are likely to have sizes mainly between
794 ~300 μm and ~2 mm. MMX will collect granular samples of more than 10 g from each
795 landing site, and is expected to obtain grains in numbers of the order of thousands or
796 more. The acquisition of a large number of regolith grains will enable us to apply
797 statistical analyses to deduce an estimate for the bulk composition of Phobos even when
798 grains exhibit a wide variation in their composition.
799
800 Analyses of returned samples will include those on grain size, shape, texture,
801 mineralogy, chemistry, isotopic composition, microscopic weathering state, chronology,
802 and so on. These measured properties will provide a set of ground truth data for the
803 global compositional map acquired by MMX remote sensing data. Sample analyses will

804 then provide us the best clue to judge the origin of Phobos as well as the processes of
805 Phobos formation in the context of material transport in the early Solar System and
806 those of Phobos surface evolution. Not only the records of shock alteration but also
807 possible extraction of exotic materials from samples are expected to provide us unique
808 information on the evolution of the Martian system including the Martian surface
809 environment.
810
811 If the majority of sampled Phobos indigenous materials are like unequilibrated
812 chondritic materials, this provides strong evidence for the capture origin of Phobos. In
813 this case, the sample is expected to be abundant in grains composed of unequilibrated
814 minerals enriched in volatile elements. Comparison of mineralogical, compositional,
815 and isotopic evidence with primitive meteorites will tell us the genetic relationships of
816 Phobos precursor and parent bodies of primitive meteorite groups in the early Solar
817 System. Using the corresponding relationships among the spectroscopic taxonomy of
818 asteroids and meteorite groups (DeMeo and Carry 2014), the source region of the
819 Phobos precursor may be estimated. Reflectance spectra of returned samples that

820 contain less altered materials may also provide better constraints on the source asteroid
821 type of the Phobos precursor. Adding to the precise impact crater statistics that will be
822 revealed by MMX close-up observations, the distribution of shock alteration ages of
823 grains will provide constraints on the major impact history of Phobos including the
824 stage of its precursor body with heliocentric orbit. With help of models for the
825 dynamical evolution of small bodies in the early Solar System, the mechanisms and
826 history of transport of H_2O-bearing bodies from the early outer Solar System to
827 terrestrial planets will be elucidated. Furthermore, processes that formed H_2O-bearing
828 bodies in the early outer Solar System may be clarified from the analyses of minerals
829 produced by aqueous alteration.
830
831 If the moon is formed by a giant impact, Phobos's indigenous materials likely have
832 textures and compositions reflecting high-temperature melting and partial vaporization
833 induced by the giant impact event. Such an event could occur with an impact velocity
834 not much larger than the escape velocity of Mars, and materials ejected into areocentric
835 orbits may inefficiently be mixed in grain-scale due to rapid solidification by efficient

836 radiative cooling (Hyodo et al. 2017). In this case, Phobos indigenous materials may
837 show isotopic and chemical compositions distributed on a mixing line connecting the
838 compositions of the proto Martian mantle and the impactor. Since the isotopic
839 compositions of elements such as oxygen are already known for Mars from the analyses
840 of Martian meteorites, the direction of the end of the mixing line points to the impactor
841 isotopic composition from which the source region of impactor may be estimated.
842 Materials that fall on isotopic end members could also tell us the chemical composition
843 of the proto Martian mantle and the impactor. The range of compositional dispersion
844 varies with the degree of material mixing, which reflects the magnitude of the moon-
845 forming impact. Crystallization ages of sample materials would constrain the timing of
846 giant impact which should be compared with the cratering record, especially of large
847 impact basins on Mars. If the impactor is found to be a volatile-rich body from the
848 sample isotopic signatures, its contribution to the development of the Martian
849 atmosphere and hydrosphere can be estimated. This should improve our understanding
850 of how Mars acquired atmosphere and water, for instance, regarding the significance or
851 insignificance of late accreting bodies. On the other hand, the composition of the proto-

852 Martian mantle estimated from sample analyses would provide us valuable information
853 on the chemical state of the early Martian mantle at the timing of the moon-forming
854 impact.
855
856 Phobos surface materials have likely been influenced by fluxes of external materials:
857 heliocentric small bodies with various sizes, impact ejecta from Mars and Deimos, and
858 ions originating from the solar wind and Martian atmosphere. Self-reproductive
859 areocentric dust particles may also continuously hit the Phobos surface. Analyses of
860 sample grains focusing on alteration by these processes would reveal how Phobos
861 surface, probably poor in endogenic activities that affect material properties, has
862 evolved in the circum-Martian environment. For example, a histogram of shock
863 alteration ages of sample grains, likely measurable by Ar-Ar dating, may provide
864 information on the history of high-speed, large-scale impacts onto Phobos along the
865 lines of similar studies for the Earth's Moon (e.g. Fernandes et al. 2013).
866 Concentrations of implanted solar wind ion in weathered samples, as well as cosmic-ray
867 exposure age, may be used to estimate the resurfacing time scale of Phobos (e.g. Nagao

et al. 2011 for Itokawa). The concentration of exotic materials would include information on the ejecta transport from Mars.

If fragments of younger impact ejecta from Mars are identified in the sample grains, they would provide information on the state of the surface environment on Mars at the timing of bedrock formation at impact site(s) (Usui et al. 2020). Their mineral assemblages, isotopic compositions, and magnetization are potential measurable proxies for the past surface environment of Mars. To make them even more valuable, the age determination of corresponding sample grains is quite important. Our capability to do this depends on grain size and mineral composition. If such measurements are successful for ejecta grains of various ages, it would significantly improve our understandings of the evolution of Mars.

Concluding Remarks

Through the exploration of the Marian moons, the MMX mission extends the

884 experience in Japanese sample return exploration for the small bodies and will
885 investigate key processes for the formation and evolution of habitable planets having
886 atmosphere and water. Close-up observations of both moons and detailed analyses of
887 samples returned from Phobos will characterize the properties of their constituent
888 materials in great detail. The mission will determine the origin of the moons which is
889 currently under debate, with models of the capture of primordial, carbonaceous
890 asteroids and the accumulation of circum-Martian debris ejected by a huge impact on
891 early Mars both being seriously considered. Also, processes for the acquisition of water,
892 organics, and volatiles from the outer Solar System by early terrestrial planets will be
893 elucidated. If the giant impact origin is the case, the differentiation state of a proto-
894 planet mantle just before the occurrence of the moon forming impact will also be a
895 study target.
896
897 Sample analyses will also extract records on the long-term evolutionary processes such
898 as continuous impactor flux and irradiation of solar wind, cosmic rays, and circum-
899 Martian plasma. For this issue, it is beneficial to conduct multidisciplinary studies with

900 remote and in-situ data including the crater population and surface reflectance of the
901 moons and the dust and plasma environment in circum-Martian space. Concurrent
902 evolutionary processes such as atmospheric circulation and escape and the possible
903 formation of dust ring and gas torus along the moons' orbits will also be study targets.
904 Ejecta materials derived from young Martian craters, if found in the returned samples,
905 will provide unique information on the Martian surface environment at the time of
906 impact and/or bedrock formation before impact.
907
908 The status of the MMX mission is now in phase B as a project of JAXA. Targeting the
909 launch in 2024, the design of spacecraft systems and instruments as well as studies of
910 spacecraft orbits, operations, and data processing including basic experiments are
911 extensively ongoing.
912

Declarations

Availability of data and materials

Not applicable.

Competing interests

The authors declare that they have no competing interests.

Funding

Through the Phase-A and Phase-B activities of MMX, our work was supported by ISAS/JAXA, NASA, CNES, DLR, and ESA. Parts of studies are also supported by Grants-in-Aid from the Japan Society for the Promotion of Science to KK, HG, and TU (18K03719, 17H06457, and 17H06459).

Authors' contributions

Overall conceptualization: KK, YK, MF, TU, and KW. Science backgrounds: GH, TI, KM, HM, TM, TN, KO, NT, and SW. Origin of Phobos and Deimos: TN and HG. Surface science and geology: HM and KW. Mars science: TI, NT, and HN. Geodesy: KM and HS. Spacecraft and instrument system: YK, HO, KO, and MO. LIDAR: HS (CIT) and KM. TENGOO/OROCHI: SK and MO. MIRS:MAB, HN, and TN,

MEGANE: DJL, TU, KO and HK, MSA:SY and NT, CMDM: MK and SS. Rover: PM and SU. Sampler: HS (jaxa) and TU. Scientific operation and orbital design: TN, HS (CIT), and HI. Sample sciences: TU, ST, and SR. All authors discussed the study and commented on the manuscript.

Acknowledgements

We thank the MMX study team, the MMX project team, the sub-science teams (Origin of Phobos and Deimos, Early Solar System Evolution, Surface Science and Geology, Mars Science, and Geodesy), the instrument teams (CMDM, C-Sampler, LIDAR, MIRS, MEGANE, MSA, ROVER, and TENGOO-OROCHI), and the working teams (Data Processing, Landing Operation, Landing Site Selection, Mission Operation, Rover Operation, and Sample Analysis) for insightful discussions for this project.

References

Barruci MA, Reess JM, Bernardi P, Doressoundiram A; Fornaiser S; Du ML, Iwata T, Nakagawa H, Nakamura T, André Y, Aoki S, Arai T, Baldit E, Beck P, Buey JT, Canalias E, Castelnau M, Charnoz S, Chaussidon M, Chapron F, Ciarletti V, Delbo M, Dubois B, Gauffre S, Gautier T, Genda H, Hassen-Khodja, R; Hervet G, Hyodo R, Imbert C, Imamura T, Jorda L, Kameda S, Kouach D, Kouyama T, Kuroda T, Kurokawa H, Lapaw L, Lasue J, Deit LL, Ledot A, Leyrat C, Ruyet BL, Matsuoka M, Merlin F, Miyamoto H, Moynier F, Tuong NN, Ogohara K, Osawa T, Parisot J, Pistre L, Quertier B, Raymond S, Rocard F, Sakanoi T., Sato TM, Sawyer E, Tache F, Trémolières S, Tsuchiya F, Vernazza P, Zeganadin D, MIRS an Imaging spectrometer for the MMX mission, This issue.

Basilevsky AT, Lorenz CA, Shingareva TV, Head JW, Ramsley KR, Zubarev AE (2014) The surface geology and geomorphology of Phobos. Planetary and Space Science, 102, 95-118. doi:10.1016/j.pss.2014.04.013

Bibring JP, Langevin Y, Mustard JF, Poulet F, Arvidson R, Gendrin A, Gondet B, Mangold N, Pinet P, Forget F, Berthe M, Bibring JP, Gendrin A, Gomez C, Gondet B,

958 Jouglet D, Poulet F, Soufflot A, Vincendon M, Combes, M, Drossart P, Encrenaz T,
959 Fouchet T, Merchiorri R, Belluci G, Altieri F, Formisano V, Capaccioni F, Cerroni P,
960 Coradini A, Fonti S, Korablev O, Kottsov V, Ignatiev N, Moroz V, Titov D, Zasova L,
961 Loiseau D, Mangold N, Pinet P, Doute S, Schmitt B, Sotin C, Hauber E, Hoffmann H,
962 Jaumann R, Keller U, Arvidson R, Mustard JF, Duxbury T, Forget F, Neukum G (2006)
963 Global mineralogical and aqueous Mars history derived from OMEGA/Mars Express
964 data. Science, 312, 400-404. doi:10.1126/science.1122659
965 Burns JA (1978) The dynamical evolution and origin of the Martian moons. Vistas in
966 Astronomy, 22, 193-210. doi:10.1016/0083-6656(78)90015-6
967 Bierhaus EB, Clark BC, Harris JW, Payne KS, Dubisher RD, Wurts DW, Hund RA,
968 Kuhns RM, Linn TM, Wood JL, May AJ, Dworkin JP, Beshore E, Lauretta DS,
969 OSIRIS-REx Team (2018) The OSIRIS-REx spacecraft and the touch-and-go sample
970 acquisition mechanism (TAGSAM). Space Science Reviews, 214, 107.
971 doi:10.1007/s11214-018-0521-6.
972 Campagnola S, Yam CH, Tsuda Y, Ogawa N, Kawakatsu Y (2018) Mission analysis for
973 the Martian Moons Explorer (MMX) mission. Acta Astronautica, 146, 409-417.

974 doi:10.1016/j.actaastro.2018.03.024

975 Canup R, Salmon J (2018) Origin of Phobos and Deimos by the impact of a Vesta-to-

976 Ceres sized body with Mars. Science advances, 4, eaar6887.

977 doi:10.1126/sciadv.aar6887

978 Chassefière E, Leblanc F (2004) Mars atmospheric escape and evolution; interaction

979 with the solar wind. Planetary and Space Science, 52, 1039-1058.

980 doi:10.1016/j.pss.2004.07.002

981 Carr MH (1996) Water on Mars. New York: Oxford University Press.

982 Cho Y, Böttger U, Rull, F, Belenguer T, Börner A, Buder M, Bunduki Y, Dietz E,

983 Hagelschuer T, Hübers H-W, Kameda S, Kopp E, Lieder M, Lopez G, Moral Inza A,

984 Paproth C, Perez Canora C, Pertenais M, Peter G, Prieto Ballesteros O, Rockstein S,

985 Rodd-Routley S, Rodriguez Perez P, Ryan C, Santamaria P, Säuberlich T, Schrandt F,

986 Schröder S, Stangarone C, Ulamec S, Usui T, Weber I, Westerdorff K, Kuramoto K, In-

987 situ science on Phobos with the Raman spectrometer for MMX (RAX) onboard the

988 MMX rover. This issue

989 Christou AA, Oberst J, Lupovka V, Dmitriev V, Gritsevich M (2014) The meteoroid

990 environment and impacts on Phobos. Planetary and Space Science, 102, 164-170.
991 doi:10.1016/j.pss.2013.07.012
992 Dauphas N, Pourmand A (2011) Hf–W–Th evidence for rapid growth of Mars and its
993 status as a planetary embryo. Nature, 473, 489-492. doi:10.1038/nature10077
994 Debaille V, Brandon AD, Yin QZ, Jacobsen B (2007) Coupled ^{142}Nd–^{143}Nd evidence
995 for a protracted magma ocean in Mars. Nature, 450, 525-528. doi:10.1038/nature06317
996 DeMeo FE, Carry B (2014) Solar System evolution from compositional mapping of the
997 asteroid belt. Nature, 505, 629-634. doi:10.1038/nature12908
998 Duxbury TC, Zakharov AV, Hoffmann H, Guinness EA (2014) Spacecraft exploration
999 of Phobos and Deimos. Planetary and Space Science, 102, 9-17.
1000 doi:10.1016/j.pss.2013.12.008
1001 Fanale FP, Salvail, JR (1990) Evolution of the water regime of Phobos. Icarus, 88, 380-
1002 395. do:10.1016/0019-1035(90)90089-R
1003 Fernandes VA, Fritz J, Weiss BP, Garrick-Bethell, I, Shuster DL (2013) The
1004 bombardment history of the Moon as recorded by ^{40}Ar-^{39}Ar chronology. Meteoritics
1005 and Planetary Science, 48, 241-269. doi:10.1111/maps.12054

1006 Fraeman AA, Murchie SL, Arvidson RE, Clark RN, Morris RV, Rivkin AS, Vilas F
1007 (2014) Spectral absorptions on Phobos and Deimos in the visible/near infrared
1008 wavelengths and their compositional constraints. Icarus, 229, 196-205.
1009 doi:10.1016/j.icarus.2013.11.021
1010 Fujiya W, Sugiura N, Hotta H, Ichimura K, Sano Y (2012) Evidence for the late
1011 formation of hydrous asteroids from young meteoritic carbonates. Nature
1012 communications, 3, 627. doi:10.1038/ncomms1635
1013 Fujiwara A, Kawaguchi J, Yeomans DK, Abe M, Mukai T, Okada T, Saito J, Yano H,
1014 Yoshikawa M, Scheeres DJ, Barnouin-Jha O, Cheng AF, Demura H, Gaskell RW,
1015 Hirata N, Ikeda H, Kominato T, Miyamoto H, Nakamura AM, Nakamura R, Sasaki S,
1016 Uesugi K (2006) The rubble-pile asteroid Itokawa as observed by Hayabusa. Science,
1017 312, 1330-1334. DOI: 10.1126/science.1125841.
1018 Genda H (2016) Origin of Earth's oceans: An assessment of the total amount, history
1019 and supply of water. Geochemical Journal, 50, 27-42. doi:10.2343/geochemj.2.0398
1020 Gendrin A, Langevin Y, Erard S (2005) ISM observation of Phobos reinvestigated:
1021 Identification of a mixture of olivine and low-calcium pyroxene. Journal of Geophysical

1022 Research: Planets, 110, E04014. doi:10.1029/2004JE002245

1023 Greeley R (1987) Release of juvenile water on Mars: Estimated amounts and timing

1024 associated with volcanism. Science, 236, 1653-1654.

1025 doi:10.1126/science.236.4809.1653

1026 Grotzinger JP, Sumner DY, Kah LC, Stack K, Gupta S, Edgar L, Rubin D, Lewis K,

1027 Schieber J, Mangold N, Milliken R, Conrad PG, DesMarais D, Farmer J, Siebach K,

1028 Calef F, Hurowitz J, McLennan SM, Ming D, Vaniman D, Crisp J, Vasavada A, Edgett

1029 KS, Malin M, Blake D, Gellert R, Mahaffy P, Wiens RC, Maurice S, Grant JA, Wilson

1030 S, Anderson RC, Beegle L, Arvidson R, Hallet B, Sletten RS, Rice M, Bell, J, Griffes J,

1031 Ehlmann B, Anderson RB, Bristow, TF, Dietrich WE, Dromart G, Eigenbrode J,

1032 Fraeman A, Hardgrove C, Herkenhoff K, Jandura L, Kocurek G, Lee S, Leshin LA,

1033 Leveille R, Limonadi D, Maki J, McCloskey S, Meyer M, Minitti M, Newsom H,

1034 Oehler D, Okon A, Palucis M, Parker T, Rowland S, Schmidt M, Squyres S, Steele A,

1035 Stolper E, Summons R, Treiman A, Williams R, Yingst A (2014) A habitable fluvio-

1036 lacustrine environment at Yellowknife Bay, Gale Crater, Mars. Science, 343.

1037 doi:10.1126/science.1242777.

1038 Gundlach B, Blum J (2013) A new method to determine the grain size of planetary
1039 regolith. Icarus, 223, 479-492. doi:/10.1016/j.icarus.2012.11.039
1040 Heavens NG, Kleinböhl A, Chaffin MS, Halekas JS, Kass DM, Hayne PO, McCleese
1041 DJ, Piqueux S, Shirley JH, Schofield JT, (2018) Hydrogen escape from Mars enhanced
1042 by deep convection in dust storms. Nature Astronomy, 2, 126-132. doi:10.1038/s41550-
1043 017-0353-4
1044 Hesselbrock AJ, Minton DA (2017) An ongoing satellite–ring cycle of Mars and the
1045 origins of Phobos and Deimos. Nature Geoscience, 10, 266-269. doi:10.1038/ngeo2916
1046 Hyodo R, Genda H, Charnoz S, Rosenblatt P (2017) On the impact origin of Phobos
1047 and Deimos. I. Thermodynamic and physical aspects. The Astrophysical Journal, 845,
1048 125. doi:10.3847/1538-4357/aa81c4
1049 Hyodo R, Kurosawa K, Genda H, Usui T, Fujita K (2019) Transport of impact ejecta
1050 from Mars to its moons as a means to reveal Martian history. Scientific reports, 9,
1051 19833. doi:10.1038/s41598-019-56139-x
1052 Hunten DM (1979) Capture of Phobos and Deimos by photoatmospheric drag. Icarus,
1053 37, 113-123. doi:10.1016/0019-1035(79)90119-2

1054 Jacobson RA (2010) The orbits and masses of the Martian satellites and the libration of
1055 Phobos. The Astronomical Journal, 139, 668-679. doi:10.1088/0004-6256/139/2/668
1056 Jakosky BM, Pepin RO, Johnson RE, Fox JL (1994) Mars atmospheric loss and isotopic
1057 fractionation by solar-wind-induced sputtering and photochemical escape. Icarus, 111,
1058 271-288. doi:10.1006/icar.1994.1145
1059 Jakosky BM, Brain D, Chaffin M, Curry S, Grebowsky J, Grebowsky J, Halekas J,
1060 Leblanc F, Lillis R, Luhmann JG, Andersson L, Andre N, Andrews D, Baird D, Baker
1061 D, Bell J, Benna M, Bhattacharyya D, Bougher S, Bowers C, Chamberlin P, Chaufray
1062 J-Y, Clarke J, Collinson G, Combi M, Connerney J, Connour K, Correira J, Crabb K,
1063 Crary F, Cravens T, Crismani M, Delory G, Dewey R, DiBraccio G, Dong C, Dong Y,
1064 Dunn P, Egan H, Elrod M, England S, Eparvier F, Ergun R, Eriksson A, Esman T,
1065 Espley J, Evans S, Fallows K, Fang X., Fillingim M, Flynn C, Fogle A, Fowler C, Fox
1066 J, Fujimoto M, Garnier P, Girazian Z, Groeller H, Gruesbeck J, Hamil O, Hanley KG,
1067 Hara T, Harada Y, Hermann J, Holmberg M, Holsclaw, G, Houston S, Inui S, Jain S,
1068 Jolitz R, Kotova A, Kuroda T, Larson D, Lee Y, Lee C, Lefevre F, Lentz C, Lo D, Lugo
1069 R, Ma Y-J, Mahaffy P, Marquette ML, Matsumoto Y, Mayyasi M, Mazelle C,

McClintock W, McFadden J, Medvedev, A, Mendillo M, Meziane K, Milby Z, Mitchell D, Modolo R, Montmessin F, Nagy A, Nakagawa H, Narvaez C, Olsen K, Pawlowski D, Peterson W, Rahmati A, Roeten K, Romanelli N, Ruhunusiri S, Russell C, Sakai S, Schneider N, Seki K, Sharrar R, Shaver S, Siskind DE, Slipski M, Soobiah Y, Steckiewicz M, Stevens MH, Stewart I, Stiepen A, Stone S, Tenishev, V, Terada N, Terada K, Thiemann E, Tolson R, Toth G, Trovato J, Vogt M, Weber T, Withers P, Xu S, Yelle R, Yiğit E, Zurek R (2018) Loss of the Martian atmosphere to space: Present-day loss rates determined from MAVEN observations and integrated loss through time. Icarus, 315, 146-157. doi:10.1016/j.icarus.2018.05.030.

Kallemeyn GW, Wasson JT (1981) The compositional classification of chondrites—I. The carbonaceous chondrite groups. Geochimica et Cosmochimica Acta, 45, 1217-1230. doi:10.1016/0016-7037(81)90145-9

Kameda et al., Design of Telecopic Nadir Imager for Geomorphology (TENGOO) and Observation of surface Reflectance by Optical CHromatic Imager (OROCHI) for the MMX mission, This issue.

Kawakatsu Y, Kuramoto K, Ogawa N, Ikeda H, Ono G, Sawada H, Imada T, Otsuki M,

1086 Otake H, Muller R, Zacny K, Satoh Y, Yamada K, Mary S, Grebenstein M, Yoshikawa
1087 K (2019) Mission definition of Martian Moons eXploration (MMX), in 70th
1088 International Astronautical Congress. IAC-19, A3, 4B, 7, x51465.
1089 Kiuchi M, Nakamura AM (2014) Relationship between regolith particle size and
1090 porosity on small bodies. Icarus, 239, 291-293. doi:10.1016/j.icarus.2014.05.029
1091 Kleine T, Touboul M, Bourdon B, Nimmo F, Mezger K, Palme H, Jacobsen SB, Yin
1092 QZ, Halliday AN (2009) Hf–W chronology of the accretion and early evolution of
1093 asteroids and terrestrial planets. Geochimica et Cosmochimica Acta, 73, 5150-5188.
1094 doi:10.1016/j.gca.2008.11.047.
1095 Kobayashi M, Krüger H, Senshu H, Wada K, Okudaira O, Sasaki S, and Kimura H
1096 (2018) In situ observations of dust particles in Martian dust belts using a large-
1097 sensitive-area dust sensor, Planetary and Space Science, 156, 41-46.
1098 doi:10.1016/j.pss.2017.12.011
1099 Kokubo E, Ida S (1998) Oligarchic growth of protoplanets. Icarus, 131, 171-178.
1100 doi:10.1006/icar.1997.5840
1101 Lawrence DJ, Peplowski PN, Beck AW, Burks MT, Chabot NL, Cully MJ, Elphic RC,

1102 Ernst CM, Fix S, Goldsten JO, Hoffer E M, Kusano H, Murchie SL, Schratz BC, Usui
1103 T, Yokley ZW (2019) Measuring the Elemental Composition of Phobos: The Mars-
1104 moon Exploration with GAmma rays and NEutrons (MEGANE) Investigation for the
1105 Martian Moons eXploration (MMX) Mission. Earth and Space Science, 6, 2605-2623.
1106 doi:10.1029/2019EA000811.
1107 Leshin LA, Mahaffy PR, Webster CR, Cabane M, Coll P, Conrad PG, Archer PD,
1108 Atreya SK, Brunner AE, Buch A, and Eigenbrode JL (2013) Volatile, isotope, and
1109 organic analysis of martian fines with the Mars Curiosity rover. Science, 341, 1238937.
1110 doi: 10.1126/science.1238937
1111 Mahaffy PR, Webster CR, Atreya SK, Franz H, Wong M, Conrad PG, Harpold D, Jones
1112 JJ, Leshin LA, Manning H, Owen T, Pepin RO, Squyres S, Trainer M, MSL Science
1113 Team (2013) Abundance and isotopic composition of gases in the Martian atmosphere
1114 from the Curiosity rover. Science, 341, 263-266. doi: 10.1126/science.1237966
1115 Michel P, Ballouz R-L, Barnouin OS, Jutzi M, Walsh KJ, May BH, Manzoni C,
1116 Richardson DC, Schwartz SR, Sugita S, Watanabe S, Miyamoto H, Hirabayashi M,
1117 Bottke WF, Connolly Jr., HC, Yoshikawa M, Lauretta DS (2020) Collisional formation

of top-shaped asteroids and implications for the origins of Ryugu and Bennu. Nature Communicationsn 11, 2665. doi:10.1038/s41467-020-16433-z

Michel P et al. The MMX rover: roving and performing in-situ surface investigations on Phobos, This issue

Mustard JF, Cooper CD, Rifkin MK (2001) Evidence for recent climate change on Mars from the identification of youthful near-surface ground ice. Nature, 412, 411-414. doi:10.1038/35086515

Murray JB, Rothery DA, Thornhill GD, Muller JP, Iliffe JC, Day T, Cook AC (1994) The origin of Phobos' grooves and crater chains. Planetary and Space Sciences, 42, 519-526. doi:10.1016/0032-0633(94)90093-0

Mumma MJ, Charnley SB (2011) The chemical composition of comets—emerging taxonomies and natal heritage. Annual Review of Astronomy and Astrophysics, 49, 471-524. doi:10.1146/annurev-astro-081309-130811

Nagao K, Okazaki R, Nakamura T, Miura YN, Osawa T, Bajo K, Matsuda S, Ebihara M, Ireland TR, Kitajima F, Naraoka H, Noguchi T, Tsuchiyama A, Yurimoto H, Zolensky ME, Uesugi M, Shirai K, Abe M, Yada T, Ishibashi Y, Fujimura A, Mukai T,

1134 Ueno M, Okada T, Yoshikawa M, Kawaguchi J (2011) Irradiation history of Itokawa
1135 regolith material deduced from noble gases in the Hayabusa samples. Science, 333,
1136 1128-1131. doi:10.1126/science.1207785
1137 Nakamura T et al. Scientific observation plan of Phobos and Deimos from MMX
1138 spacecraft, This issue.
1139 Nishiizumi K, Arnold JR, Kohl CP, Caffee MW, Masarik J, Reedy RC (2009) Solar
1140 cosmic ray records in lunar rock 64455. Geochimica et Cosmochimica Acta, 73, 2163-
1141 2176. doi:10.1016/j.gca.2008.12.021
1142 Pang KD, Rhoads JW, Lane AL, Ajello JM (1980) Spectral evidence for a
1143 carbonaceous chondrite surface composition on Deimos. Nature, 283, 277-278.
1144 doi:10.1038/283277a0
1145 Pang KD, Pollack JB, Veverka J, Lane AL, Ajello JM (1978) The composition of
1146 Phobos: Evidence for carbonaceous chondrite surface from spectral analysis. Science,
1147 199, 64-66. doi:10.1126/science.199.4324.64
1148 Pollack JB, Burns JA, Tauber ME (1979a) Gas drag in primordial circumplanetary
1149 envelopes: A mechanism for satellite capture. Icarus, 37, 587-611. doi:10.1016/0019-

1035(79)90016-2

Pollack JB, Colburn DS, Flasar FM, Kahn R, Carlston CE, Pidek D (1979b) Properties and effects of dust particles suspended in the Martian atmosphere. Journal of Geophysical Research: Solid Earth, 84, 2929-2945. doi:10.1029/JB084iB06p02929

Poppe AR, Curry SM (2014) Martian planetary heavy ion sputtering of Phobos. Geophysical Research Letters, 41, 6335-6341. doi:10.1002/2014GL061100

Ramsley KR, Head, JW (2013) Mars impact ejecta in the regolith of Phobos: Bulk concentration and distribution. Planetary and Space Science, 87, 115-129. doi:10.1016/j.pss.2013.09.005

Rivkin AS, Brown RH, Trilling DE, Bell Iii JF, Plassmann JH (2002) Near-infrared spectrophotometry of Phobos and Deimos. Icarus, 156, 64-75. doi:10.1006/icar.2001.6767

Rosenblatt P (2011) The origin of the Martian moons revisited. The Astronomy and Astrophysics Review, 19, 44. doi:10.1007/s00159-011-0044-6

Rosenblatt P, Charnoz S, Dunseath KM, Terao-Dunseath M, Trinh A, Hyodo R, Genda H, Toupin S (2016) Accretion of Phobos and Deimos in an extended debris disc stirred

1166 by transient moons. Nature Geoscience, 9, 581-583. doi:10.1038/ngeo2742

1167 Senshu H et al. Development of LIDAR onboard MMX, This issue

1168 Soter S (1971) The dust belts of Mars. Report of Center for Radiophysics and Space

1169 Research, 462.

1170 Sugita S, Honda R, Morota T, Kameda S, Sawada H, Tatsumi E, Yamada M, Honda C,

1171 Yokota Y, Kouyama T, Sakatani N, Ogawa K, Suzuki H, Okada T, Namiki N, Tanaka

1172 S, Iijima Y, Yoshioka K, Hayakawa M, Cho Y, Matsuoka M, Hirata N, Hirata N,

1173 Miyamoto H, Domingue D, Hirabayashi M, Nakamura T, Hiroi T, Michikami T, Michel

1174 P, Ballouz R-L, Barnouin OS, Ernst CM, Schröder SE, Kikuchi H, Hemmi R, Komatsu

1175 G, Fukuhara T, Taguchi M, Arai T, Senshu H, Demura H, Ogawa Y, Shimaki Y,

1176 Sekiguchi T, Müller TG, Hagermann A, Mizuno T, Noda H, Matsumoto K, Yamada R,

1177 Ishihara Y, Ikeda H, Araki H, Yamamoto K, Abe S, Yoshida F, Higuchi A, Sasaki S,

1178 Oshigami S, Tsuruta S, Asari K, Tazawa S, Shizugami M, Kimura J, Otsubo T, Yabuta

1179 H, Hasegawa S, Ishiguro M, Tachibana S, Palmer E, Gaskell R, Le Corre L, Jaumann

1180 R, Otto K, Schmitz N, Abell PA, Barucci MA, Zolensky ME, Vilas F, Thuillet F,

1181 Sugimoto C, Takaki N, Suzuki Y, Kamiyoshihara H, Okada M, Nagata K, Fujimoto M,

1182 Yoshikawa M, Yamamoto Y, Shirai K, Noguchi R, Ogawa N, Terui F, Kikuchi S,

1183 Yamaguchi T, Oki Y, Takao Y, Takeuchi H, Ono G, Mimasu Y, Yoshikawa K,

1184 Takahashi T, Takei Y, Fujii A, Hirose C, Nakazawa S, Hosoda S, Mori O, Shimada T,

1185 Soldini S, Iwata T, Abe M, Yano H, Tsukizaki R, Ozaki M, Nishiyama K, Saiki T,

1186 Watanabe S, Tsuda Y (2019) The geomorphology, color, and thermal properties of

1187 Ryugu: Implications for parent-body processes. Science, 364, eaaw0422.

1188 doi:10.1126/science.aaw0422

1189 Tolson RH, Duxbury TC, Born GH, Christensen EJ, Diehl RE, Farless D, Hildebrand

1190 CE, Mitchell RT, Molko PM, Morabito LA, Palluconi FD, Reichert RJ, Taraji H,

1191 Veverka J, Neugebauer G, Findlay JT (1978) Viking first encounter of Phobos:

1192 Preliminary results. Science, 199, 61-64. doi:10.1126/science.199.4324.61

1193 Thomas PC (1989) The shapes of small satellites. Icarus, 77, 248-274.

1194 doi:10.1016/0019-1035(89)90089-4

1195 Thomas PC (1993) Gravity, tides, and topography on small satellites and asteroids:

1196 Application to surface features of the Martian satellites. Icarus, 105, 326-344.

1197 doi:10.1006/icar.1993.1130

1198 Thomas PC, Adinolfi D, Helfenstein P, Simonelli D, Veverka J (1996) The surface of
1199 Deimos: Contribution of materials and processes to its unique appearance. Icarus, 123,
1200 536-556. doi:10.1006/icar.1996.0177
1201 Usui T, Bajo KI., Fujiya W, Furukawa Y, Koike M, Miura YN, Sugawara H, Tachibana
1202 S, Takano Y, Kuramoto K (2020) The importance of Phobos sample return for
1203 understanding the Mars-moon system. Space Science Reviews, 216, 49.
1204 doi:10.1007/s11214-020-00668-9
1205 Villanueva GL, Mumma MJ, Novak RE, Käufl HU, Hartogh P, Encrenaz T, Tokunaga
1206 A, Khayat A, Smith MD (2015) Strong water isotopic anomalies in the martian
1207 atmosphere: Probing current and ancient reservoirs. Science, 348, 218-221.
1208 doi:10.1126/science.aaa3630
1209 Veverka J, Duxbury TC (1977) Viking observations of Phobos and Deimos:
1210 Preliminary results. Journal of Geophysical Research, 82, 4213-4223.
1211 doi:10.1029/JS082i028p04213
1212 Walsh KJ, Morbidelli A, Raymond SN, O'Brien DP, Mandell AM (2011) A low mass
1213 for Mars from Jupiter’s early gas-driven migration. Nature, 475, 206-209.

1214 doi:10.1038/nature10201

1215 Warren PH (2011) Stable-isotopic anomalies and the accretionary assemblage of the

1216 Earth and Mars: A subordinate role for carbonaceous chondrites. Earth and Planetary

1217 Science Letters, 311, 93-100. doi:10.1016/j.epsl.2011.08.047

1218 Wasson JT, Kallemeyn GW (1988) Compositions of chondrites. Philosophical

1219 Transactions of the Royal Society of London. Series A, Mathematical and Physical

1220 Sciences, 325, 535-544. doi:10.1098/rsta.1988.0066

1221 Watanabe S, Hirabayashi M, Hirata N, Hirata N, Noguchi R, Shimaki Y, Ikeda H,

1222 Tatsumi E, Yoshikawa M, Kikuchi S, Yabuta H, Nakamura T, Tachibana S, Ishihara Y,

1223 Morota T, Kitazato K, Sakatani N, Matsumoto K, Wada K, Senshu H, Honda C,

1224 Michikami T, Takeuchi H, Kouyama T, Honda R, Kameda S, Fuse T, Miyamoto H,

1225 Komatsu G, Sugita S, Okada T, Namiki N, Arakawa M, Ishiguro M, Abe M, Gaskell R,

1226 Palmer E, Barnouin OS, Michel P, French AS, McMahon JW, Scheeres DJ, Abell PA,

1227 Yamamoto Y, Tanaka S, Shirai K, Matsuoka M, Yamada M, Yokota Y, Suzuki H,

1228 Yoshioka K, Cho Y, Tanaka S, Nishikawa N, Sugiyama T, Kikuchi H, Hemmi R,

1229 Yamaguchi T, Ogawa N, Ono G, Mimasu Y, Yoshikawa K, Takahashi T, Takei Y, Fujii

1230 A, Hirose C, Iwata T, Hayakawa M, Hosoda S, Mori O, Sawada H, Shimada T, Soldini
1231 S, Yano H, Tsukizaki R, Ozaki M, Iijima Y, Ogawa K, Fujimoto M, Ho T-M, Moussi
1232 A, Jaumann R, Bibring J-P, Krause C, Terui F, Saiki T, Nakazawa S, Tsuda Y (2019)
1233 Hayabusa2 arrives at the carbonaceous asteroid 162173 Ryugu—A spinning top–shaped
1234 rubble pile. Science, 364, 268-272. doi:10.1126/science.aav8032
1235 Yokota S, Saito Y, Asamura K, Tanaka T, Nishino MN, Tsunakawa H, Shibuya H,
1236 Matsushima M, Shimizu H, Takahashi F, Fujimoto M, Mukai T, Terasawa T (2009) First
1237 direct detection of ions originating from the Moon by MAP-PACE IMA onboard
1238 SELENE (KAGUYA). Geophysical Research Letters, 36. doi:10.1029/2009GL038185
1239 Yokota S, Terada N, Matsuoka A, Murata N, Saito Y, Delcourt D; Futaana Y, Seki K,
1240 Schaible MJ, Asamura K, Kasahara S, Nakagawa H, Nishino MN, Nomura R, Keika K,
1241 Harada Y, Imajo S, In situ observations of ions and magnetic field around Phobos: The
1242 Mass Spectrum Analyzer (MSA) for the Martian Moons eXploration (MMX) mission,
1243 This issue.
1244 Zellner BH, Capen RC (1974) Photometric properties of the Martian satellites. Icarus,
1245 23, 437-444. doi:10.1016/0019-1035(74)90062-1
1246

Figure titles and legends

Figure 1. The current design of spacecraft system configuration. (Top) From left to right, propulsion, exploration, and return modules. (Bottom) On-orbit configuration. The size of a solar panel is 2.4 m × 4.4 m. (C) JAXA

Figure 2. The mission profile of MMX. See text for details.

Figure 3. Planned observational orbits around Phobos. Quasi-satellites orbits (QSOs) are drawn in the Phobos fixed frame with Phobos at the center taking the xy-plane and the x-axis direction to be the Phobos orbital plane and the opposite direction to Mars, respectively. Top: QSOs confined in the xy-plane. Bottom: 3D QSOs.

Figure 4. Outline of the tentative operation plan of MMX. The two panels are based on changes in the duration of eclipses by Mars and Phobos (top) and those in the configuration of Mars relative to the Sun and Earth (bottom), respectively. For eclipse duration estimates, a QSO-L orbit is assumed. CO: check out, H: QSO-H, M: QSO-M,

1263 LA: QSO-LA, LB: QSO-LB, LC: QSO-LC, LSS: landing site selection, TD: touch

1264 down, DM: Deimos. Courtesy of Nakamura T and Ikeda H.

1265

Tables

Table 1 Major properties of the Martian moons

Parameters	Phobos	Deimos	Ref.
Mass [kg][1)]	$1.0626\pm0.0006\times10^{16}$	$1.51\pm0.04\times10^{15}$	1
Size [km][2)]	$13.3\times11.1\times9.1$	$7.5\times6.1\times5.2$	2
Volume [km^3]	5621 ± 154	997 ± 49	2
Mean density [g/cm^3]	1.89 ± 0.05	1.51 ± 0.07	Mass/Vol.
Semi-major axis [Mars radius]	2.76	6.92	3
Eccentricity	0.0151	0.00033	3
Inclination [°][3)]	1.093	1.791	3
Geometric albedo	0.07 ± 0.012	0.068 ± 0.007	4, 5

1) GM values are converted to mass by adopting G=6.67430×10^{-11} m^3 kg^{-1} s^{-2}, 2) semiaxes of the approximated triaxial ellipsoids, 3) relative to the Laplace plane

1. Jaconson (2020), 2. Thomas (1989), 3. JPL Solar System Dynamics, https://ssd.jpl.nasa.gov/, 4. Zellner and Capen (1974), 5. Thomas et al. (1996)

Table 2. Observational pros (P) and cons (C) for hypotheses for the origin of the Martian Moons.

Evaluation item	Asteroid capture		Giant impact	
Low surface reflectance with reddening spectra lacking clear silicate absorption features	P	This resembles D-type asteroids, and so is regarded as strong grounds for the asteroid capture theory.	N	No absorption feature indicative of ejected Martian source materials is identified so far. Note that this might be masked by strong impact alteration or mixing of materials from the impactor.
Small orbital eccentricity (e) and inclination (I) relative to the Martian equatorial plane	C	It seems difficult, especially for Deimos, for these orbits to evolve from a large e and random I through tidal friction alone.	P	This is naturally explained if the giant impact introduces most of the spin angular momentum of Mars associated with the generation of a Moon-forming debris disk.
Low-mass objects orbiting within and beyond the co-rotation radius (r_c) with Martian rotation	N	Tidal evolution theory predicts Phobos should be formed just inside r_c, making the conditions for capture severe. A similar difficulty exists to explain Deimos's orbital radius unless some frictional medium such as a gas envelope extended to a large distance.	C	The formation of Deimos outside of r_c requires a large disk mass, resulting in the formation of a massive inner moon. Tidal friction could eventually lead such a moon to falling onto Mars but geologic evidence for such an impact is yet unidentified.

N: neutral.

1273 Table 3. Scientific mission objectives and requirements of MMX

1274 (MO: mission objectives, MR: mission requirements, Priority: SS=very high, S=high, A=valuable)

Goal 1: Clarify the origins of the Martian moons and constrain processes for planetary formation and material transport in the region connecting the inner and outer Solar System.		
Medium objective 1.1 Reveal whether Phobos originated as a captured asteroid or resulted from a giant impact		
MO1.1.1: Spectroscopically reveal the surface-layer distribution of the materials that make up Phobos with the spatial resolution required for the scientific evaluation of sampling points and geological structures, thereby constraining Phobos' origin.	SS	MR1.1.1: To grasp the distribution of the constituent materials of Phobos, material distributions of hydrous minerals and other related minerals should be obtained spectroscopically for main parts of the full body in correspondence with its topography (at horizontal spatial resolutions of 20 m or better) and in a radius of 50 m or more around the sampling point (at spatial resolutions of 1 m or better). Also, the mean global Si/Fe ratio, etc., of the moon should be determined to within an accuracy of 20%.
MO1.1.2: Identify the major components of constituent materials from samples collected on Phobos' surface as Phobos indigenous materials that retain records of their formation, strongly constraining their origins from isotopic ratios, etc.	SS	MR1.1.2: To constrain the origins of Phobos, paying attention to the diversity and representativeness of Phobos' surface, record the occurrence of and collect at least 10 g of particulate samples (Phobos samples), including samples 2 cm below the surface. Also, identify main sample components as moon-indigenous materials that were constituent materials at the time of formation, and measures their texture and mineral, elemental, and isotopic composition (oxygen, chromium, etc.) with sufficient accuracy to allow the specification of the moon's origins.
MO1.1.3: Obtain information such as molecular release rates and mass distribution related to the presence of ice in Phobos, investigate the presence or absence of density contrasts on Phobos' surface, and constrain Phobos' origin independently of MO1.1.1 and MO1.1.2.	S	MR1.1.3 : To constrain the origin of Phobos from its internal structure, (1) measure the molecular release rate from internal ice at a detection limit of fewer than 10^{22} molecules/s, (2) investigate the presence or absence of inhomogeneity in the density structure due to localization of ice exceeding 10% of Phobos' mass, and (3) investigate the presence or absence of density veriation near the surface layer.
Medium objective 1.2a [If Phobos is determined to be a captured asteroid] Elucidate the composition and migration process of primitive materials supplied to the region of terrestrial planets and constrain the initial conditions of Martian surface evolution		
MO1.2a.1: By constraining the formation of primitive materials in the Solar System and primitive bodies in the vicinity of the snow line from a materials science perspective, and by estimating the Phobos capture process, constrain the initial conditions for the process of celestial body migration and evolution of the Martian surface in the early Solar System.	S	MR1.2a: To constrain the initial evolution of Solar System materials and volatile element supply, analyze texture, element and isotope composition, formation age, etc., of moon-indigenous materials in Phobos samples with the necessary accuracy and also extract information related to organic matter and hydrous minerals. Also, elucidate collision environments before and after moon capture from the age distribution of impact metamorphisms in the collected sample and measurements of crater distributions on the moon surface.
Medium objective 1.2b [If Phobos is determined to originate from a giant impact] Elucidate giant impact and moon formation processes in the terrestrial planetary region and evaluate its influence on the early evolutionary process of Mars		
MO1.2b.1: For Phobos indigenous materials, identify primitive Martian components (Mars-originating components) ejected by a giant impact and components of the impactor body, clarify their features, estimate the scale and age of the impact, and constrain celestial migration and planetary formation processes in the terrestrial planetary region.	S	MR1.2b: To constrain the process of a giant impact, analyze the texture, elemental and isotopic composition, metamorphic age, etc., of moon-indigenous materials in the Phobos sample with sufficient accuracy, and estimate the peak temperature, timing of the collision, and the mixing ratio of components from primitive Mars and the impacting body. Also, restrict the mixing ratio of both components across the entire moon from measurements of the Si/Fe ratio, etc.
Medium objective 1.3 Place new constraints on Deimos' origin		
MO1.3.1: Elucidate the surface distribution of materials composing Deimos through spectroscopy with the spatial resolution necessary for grasping its geological structures and compare this with Phobos.	S	MR1.3: To grasp the distribution of constituent materials of Deimos, from spectroscopic information, clarify the surface distribution of hydrous minerals and other related minerals corresponding to its topography at characteristic parts of the moon with a horizontal spatial resolution of 100 m or better.
Goal 2 From the viewpoint of the Martian moons, clarify the driving mechanism of the transition of the Mars-moon system, and add new knowledge to the evolution history of Mars.		
Medium objective 2.1 Obtain a basic description of the elementary processes of surface evolution for moons in the circum-Martian environment		

MO2.1.1: Identify weathering and evolutionary processes (impact frequency, degree of gardening, and space weathering processes) in surface-layer regolith specific to the Martian moons as compared to asteroids.	SS	MR2.1: To know the surface evolution processes of Martian moons, (1) observably constrain the circum-moons environment, (2) grasp Phobos' geological features and surface structures (craters, boulders, thickness and deposition state of the regolith layer) at horizontal spatial resolutions of 20 m or better, and (3) elucidate the state of space weathering and metamorphism in Phobos samples.
Medium objective 2.2 Add new findings and constraints on the history of changes in the Martian surface		
MO2.2.1: Search returned samples of the Phobos surface for materials ejected from Mars after the formation of Phobos and constrain the chemical state of the Martian surface layer and its transition if suitable samples are present.	A	MR2.2.1: To constrain the chemical state and transition of the surface layer of Mars, search a Phobos sample of 10 g or more for materials (ejecta) from Mars from after moon formation, and, if appropriate samples are present, clarify features such as isotopic composition, formation age, and remanent magnetization.
MO2.2.2: Place constraints on the amount of atmospheric escape through the history of Mars from composition ratios and isotopic ratios in the current escaping atmosphere.	A	MR2.2.2: To constrain the amount of atmospheric escape through the history of Mars, measure composition ratios and isotopic ratios of the main components of ions escaping from the current Martian atmosphere to an accuracy within 50%.
Medium objective 2.3 Constrain the mechanisms of material circulation in the Martian atmosphere affecting the transitions in the Martian climate		
MO2.3.1: Impose constraints on dust and water transport processes in the Martian atmosphere and between the atmosphere and the surface through observations of the temporal changes in dust storms and the global distributions of water vapor and clouds.	A	MR2.3: To constrain transport processes for dust and water near the Martian surface, continuous observations of the mid-to low-latitude distributions of dust storms, ice clouds, and water vapor in the Martian atmosphere are performed from high altitude equatorial orbit in different seasons to within 1-hour time resolutions.

1277 Table 4. Instruments onboard MMX for scientific observations

Name: function	Major specifications	Roles		
		Moons' origin	Sampling assist	Mars system
LIDAR:[1] laser altimeter	• Laser wavelength 1064 nm • Ranging distance: 100 m - 100 km • Ranging resolution: < 22 m @ 100 km • Footprint 50 m from 100 km altitude	Characterization of geologic structures and bedrock exposed areas	Selection and characterization of sampling sites in terms of safety for landing, geologic context, and representativeness as pieces of bedrock	Measurement of surface morphology for the geologic history of the moons
TENGOO:[2] telescopic camera	• FOV: 1.1° × 0.82° • Wavelength: a part of visible light • Spatial resolution: ~40 cm @ 20 km alt.			
OROCHI:[3] wide-angle multiband camera	• FOV: 66° × 53° • Wavelength (width): 390 (50), 480 (30), 550 (30), 650 (10), 700 (10), 800 (40), 950 (60) nm, and 400 - 900 nm (monochromatic) • Spatial resolution: 20 m @ 20 km alt., 10 cm for an area of 100 × 100 m^2 around landing sites, 1 mm for an area of 1 × 1 m^2 around sampling sites	Determination of global surface composition (Hydrous minerals, Fe/Si, H_2O release rate, etc.)		Observation of H_2O and dust circulation in the Martian climate system
MIRS:[4] near infrared spectrometer	• FOV:3.3 ° (in the direction of spectrometer slit) • Wavelength: 0.9 - 3.6 μm • Spectral sampling: 10 nm • Spatial resolution: < 20 m @ 20 km alt.			
MSA:[5] ion mass spectrometer	• Geometric factor: $\geq 10^4$ cm^2 sr eV/eV • Ion energy: ~5 eV/q-~30 keV/q, Energy resolution: ΔE/E ~ 10% • Ion mass: 1 - 100 amu, Mass resolution: M/ΔM > 100			Searching for the gas torus and escaping Martian atmosphere
MEGANE:[6] gamma-ray and neutron spectrometer	• Gamma-ray energy: 0.4-8 MeV with energy resolution: < 5.1 keV (FWHM) @ 1454 keV • Neutron energy: thermal (0.01 eV - 0.5 eV), epithermal (0.5 eV - 0.5 MeV), fast (0.5 MeV - 7 MeV)			(not assigned)
MMX Rover: solar powered rover	• Laser Raman spectrometer • Thermal radiometer • Navigation cameras • Wheel cameras	In situ measurement of mineralogy and physical properties of regolith		
CMDM:[7] dust counter	• Dust size: > 10 - 20 μm • Dust velocity: > 0.16 km/s	Detecting dust flux and ring to reveal the weathering process on the moons' surface by micrometeoroid bombardments		

1278 1) LIght DEtection and Ranging, 2) TElescopic Nadir imager for GeOmOrphology (name after long-nosed goblin in Japanese folklore), 3) Optical
1279 RaidOmeter composed of CHromatic Imagers (after giant snake with eight heads in Japanese folklore), 4) MMX InfraRed Spectrometer, 5) Mass
1280 Spectrum Analyzer, 6) Mars moons Exploration with GAmma rays and Neutrons (after eyeglasses in Japanese), 7) Circum Martian Dust Monitor

Figures

Figure 1

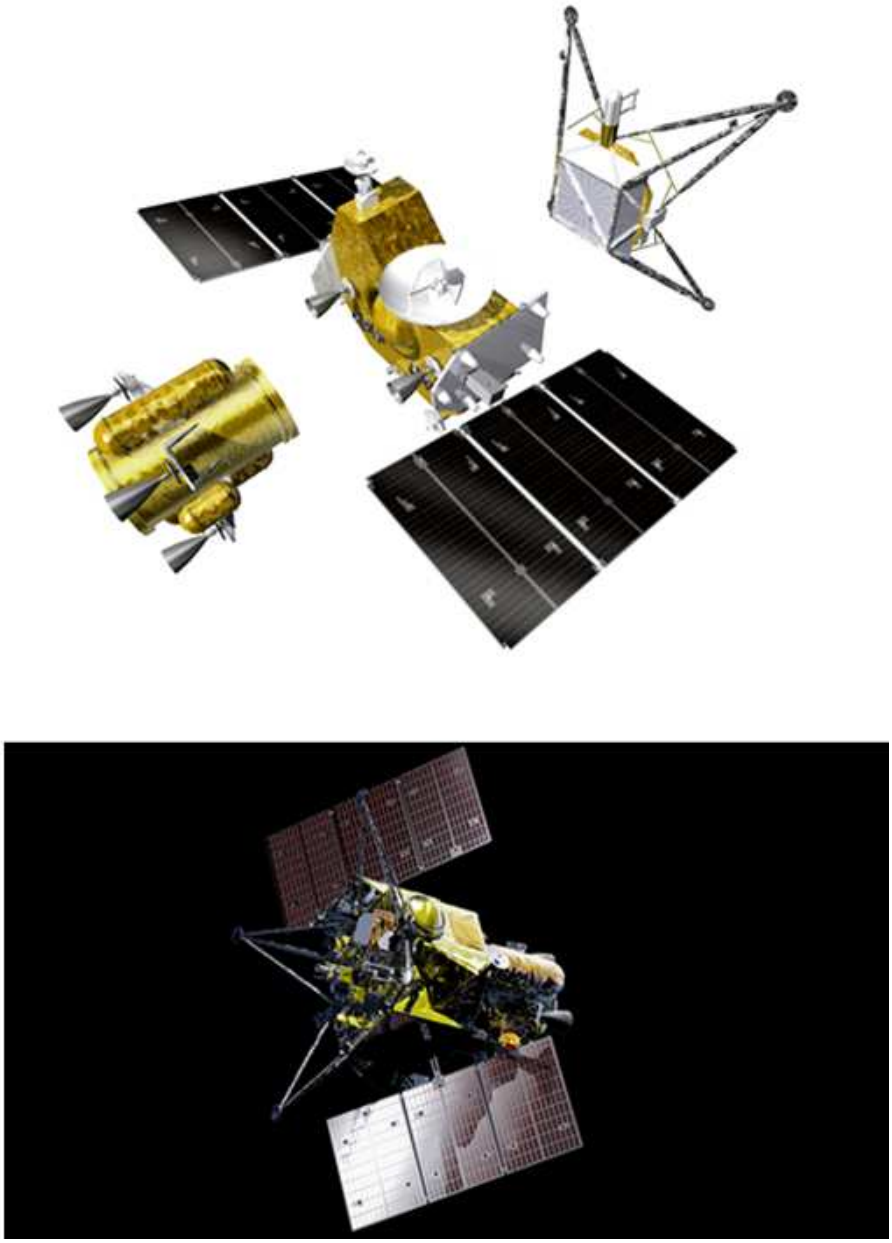

Figure 1

The current design of spacecraft system configuration. (Top) From left to right, propulsion, exploration, and return modules. (Bottom) On-orbit configuration. The size of a solar panel is 2.4 m × 4.4 m. (C) JAXA

Figure 2

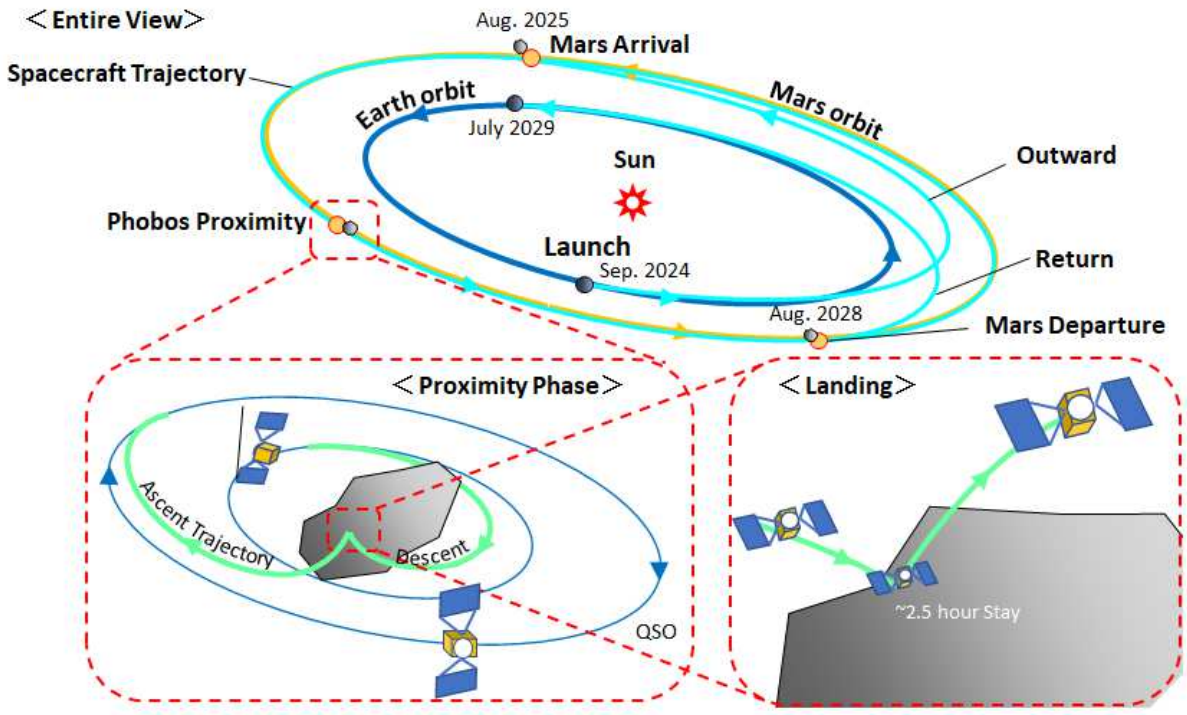

Figure 2

The mission profile of MMX. See text for details.

Figure 3

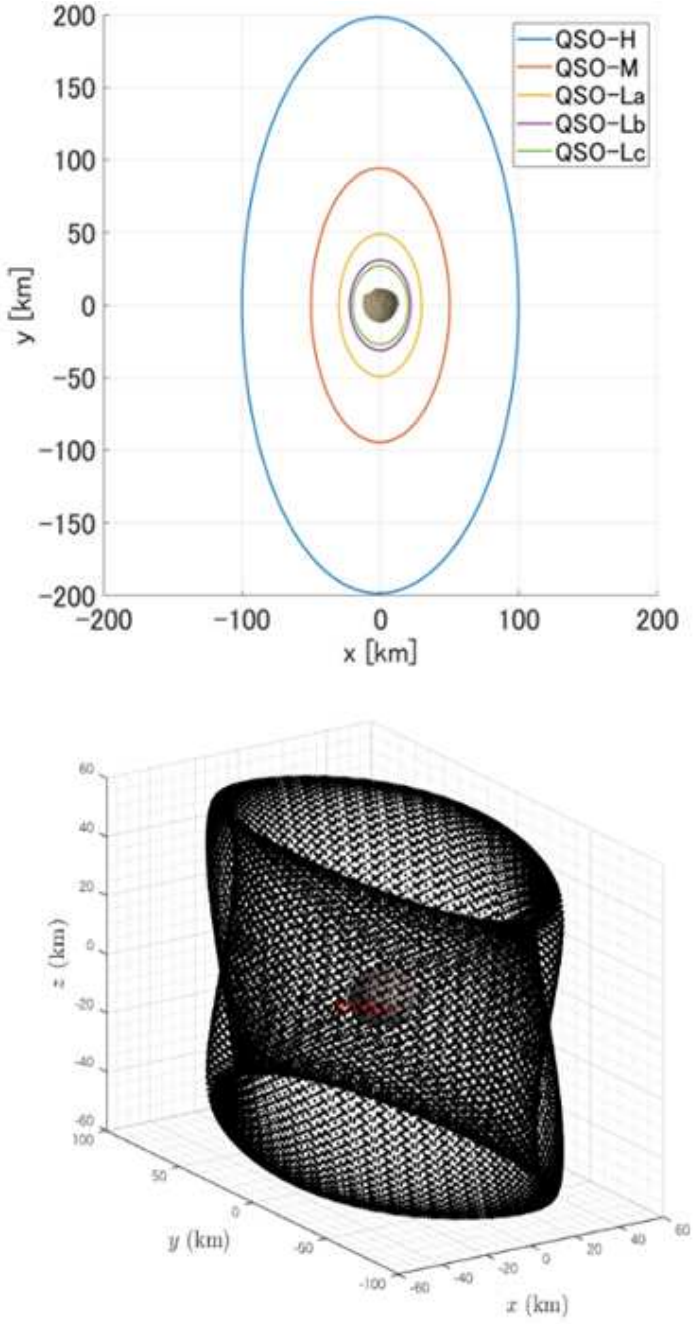

Figure 3

Planned observational orbits around Phobos. Quasi-satellites orbits (QSOs) are drawn in the Phobos fixed frame with Phobos at the center taking the xy-plane and the x-axis direction to be the Phobos orbital plane and the opposite direction to Mars, respectively. Top: QSOs confined in the xy-plane. Bottom: 3D QSOs.

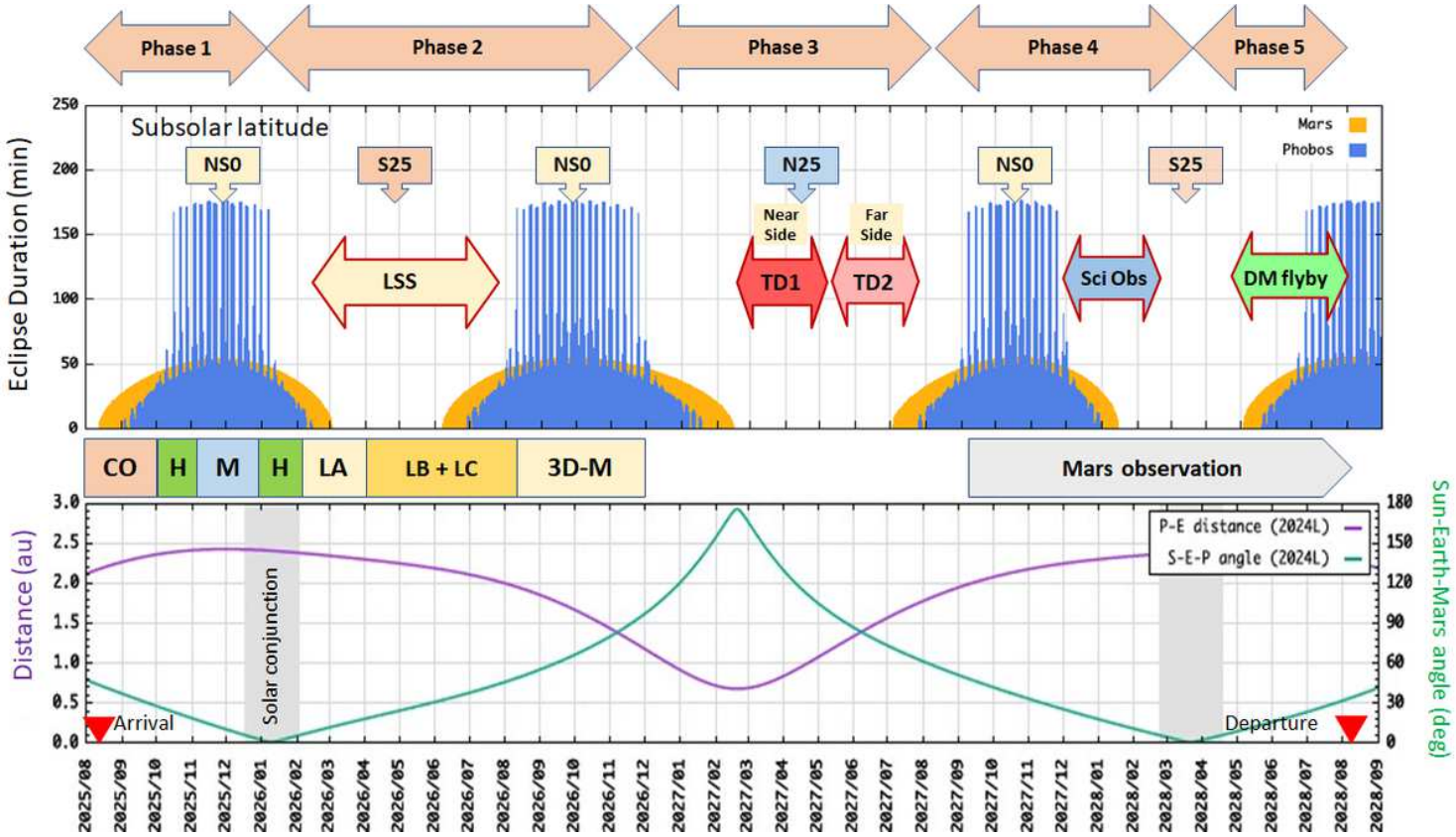

Figure 4

Outline of the tentative operation plan of MMX. The two panels are based on changes in the duration of eclipses by Mars and Phobos (top) and those in the configuration of Mars relative to the Sun and Earth (bottom), respectively. For eclipse duration estimates, a QSO-L orbit is assumed. CO: check out, H: QSO-H, M: QSO-M, LA: QSO-LA, LB: QSO-LB, LC: QSO-LC, LSS: landing site selection, TD: touch down, DM: Deimos. Courtesy of Nakamura T and Ikeda H.

Supplementary Files

This is a list of supplementary files associated with this preprint. Click to download.

- graphicalabstract.png